Chapter 6: Towards the Elucidation of the Activation of Cisplatin in Anticancer Treatment

Jaroslav V. Burda[a], Jiří Šponer[b,c] and Jerzy Leszczynski[d]

[a]*Department of Chemical Physics and Optics, Faculty of Mathematics and Physics, Charles University, Ke Karlovu 3, 121 16 Prague 2, Czech Republic*

[b]*Institute of Biophysics, Academy of Sciences of the Czech Republic, Královopolská 135, 612 65 Brno, Czech Republic*

[c]*Institute of Organic Chemistry and Biochemistry, Academy of Sciences of the Czech Republic, Flemingovo náměstí 2, 166 10 Prague 6, Czech Republic*

[d]*Computational Center for Molecular Structure and Interactions, Department of Chemistry, Jackson State University, Jackson, Mississippi 39217, USA*

Abstract

The first step in biological activity of cisplatin, one of the most efficient anticancer drugs, involves the hydration process. This chapter reviews the results of theoretical studies concerning the activation of cisplatin and its analogs. The complexity of the studied phenomena requires application of different theoretical tools. The energetic description of the extended hydration scheme was performed for the square-planar Pt(II) and Pd(II) complexes. High-accuracy methodology was adopted for the predictions of their heats of reactions. Molecular mechanism of the ligand replacement by

water molecules was investigated using the supermolecular approach. In this model the reactant metal complex was examined together with an additional water molecule. Based on such approach, not only thermodynamical but also kinetical parameters can be determined. The CCSD(T) computational level was used for the determination of the reaction energy profiles. Despite the high accuracy, it was found that the obtained results do not sufficiently match the experimental data. This causes the necessity of the improvement of the gas-phase calculations using the implicit solvent in the polarizable continuum model. The COSMO method was applied on the B3LYP-reoptimized geometries and was augmented by the CCSD(T) single point calculations. These final results are in excellent accord with both the experimental data as well as other calculated values.

1. The Effect of Cisplatin in the Cell

Cisplatin (cis-dichlorodiammineplatinum cisDDP) belongs to one of the most frequently explored platinum compounds since Rosenberg's discovery of its anticancer activities.[1] It was found that cisplatin makes a bridge connection between two (usually) adjacent guanine bases in DNA predominately forming 1,2–intrastrand GpG complexes (about 65% of the occurrences). Some other intrastrand coordinations occur less frequently, namely with the 1,2-d(ApG) and the 1,3-d(GpXpG) base sequences. However, coordination to the 1,2-d(ApA) or the 1,2-d(GpA) fragment was observed only very rarely.

The high mobility group (HMG) proteins can recognize the bend on the platinated DNA α-helix and bind to it.[2] Structures of such Pt-DNA-HMG complexes were solved recently based on crystallographic data.[3-5]

Cisplatin can also interact with other molecules in a cellular environment, like peptide structures[6-10] or RNA's.[11] The main cisplatin targets, before nucleus is reached, are side chains of amino acids on the surface of proteins or peptides like glutathione.[12,13] A considerable amount of effort has been devoted to the study of these interactions. Sulphur-containing amino acids like methionine and cysteine were frequently considered.[14-16] Some attention was also paid to interactions of cisplatin with N-side chains of amino acids like histidine,[17-20] arginine or amides of aspartic[21] and glutamic acids[22] as well as other amino acids.[23,24]

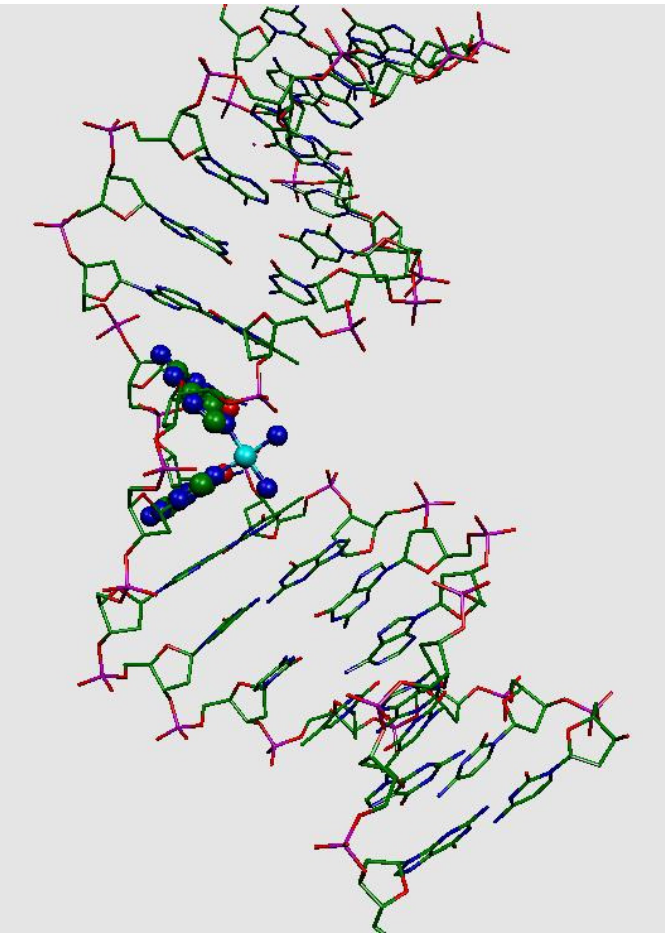

Figure 1. The X-ray structure of the cisplatin adduct to dodecamer sequence of DNA d(CCTCTG*G*TCTCC)/d(GGAGACCAGAGG) (pdb structure 1a84).[136]

2. Experimental Data on Cisplatin Hydration

Before all of the above mentioned interactions can occur, cisplatin undergoes the hydration process. Many studies have been devoted to the

thermodynamics and kinetics of cisplatin hydration. As to the experimental works, the thermodynamic data for the replacement of the chloride ligand by water molecules were reported by Hindmarch et al.[25] for both the hydration steps:

$$cis-[Pt(NH_3)_2Cl_2]+H_2O \underset{}{\overset{K_1}{\rightleftharpoons}} Cl^- + cis-[Pt(NH_3)_2Cl(H_2O)]^+ \quad (1)$$
$$cis-[Pt(NH_3)_2Cl(H_2O)]^+ + H_2O \underset{}{\overset{K_2}{\rightleftharpoons}} Cl^- + cis-[Pt(NH_3)_2(H_2O)_2]^{2+}$$

The values of equilibrium constants $\log K_1 = -2.19$ and $\log K_2 = -3.53$ in 1.0 M $NaClO_4$ solution were found. Arpalahti et al.[26,27] determined the equilibrium constants for analogous processes of transplatin. Slightly smaller hydration constants were reported: $\log K_1 = -2{,}92$ and $\log K_2 = -4{,}41$ in more diluted 0.1 M $NaClO_4$ solution. Due to their dependence on the pH value of the environment, the hydrated complexes can be subsequently stabilized by deprotonation of the aqua ligands.[28] This means that in the basic solutions (with pH > 7) the activity of the platinum complexes will be reduced:

$$cis-[Pt(NH_3)_2Cl(H_2O)]^+ \underset{}{\overset{K_{a3}}{\rightleftharpoons}} H^+ + cis-[Pt(NH_3)_2Cl(OH)]$$
$$cis-[Pt(NH_3)_2(H_2O)_2]^{2+} \underset{}{\overset{K_{a1}}{\rightleftharpoons}} H^+ + cis-[Pt(NH_3)_2(H_2O)(OH)]^+$$
$$cis-[Pt(NH_3)_2(H_2O)(OH)]^+ \underset{}{\overset{K_{a2}}{\rightleftharpoons}} H^+ + cis-[Pt(NH_3)_2(OH)_2] \quad (2)$$

The values of these pK_a were determined for both cisplatin and transplatin in many laboratories.[29-32] Approximate values of individual pK_a based on several measurements can be estimated as $pK_{a1} = 5.5$, $pK_{a2} = 7.3$, and $pK_{a3} = 6.6$ for cisplatin. The estimations for transplatin are $pK_{a1} = 4.4$, $pK_{a2} = 7.3$, and $pK_{a3} = 5.6$. It can be noticed that the hydrated transplatin deprotonates in the first step more readily (or at lower pH) than cisplatin. The same is also true for the corresponding singly-hydrated platinum complexes (pK_{a3}).

The kinetic parameters of the hydration processes were also studied. It is widely accepted that the substitution reactions occur predominately by an associative mechanism in the case of Pt(II) and transition metals universally.[33] Despite the fact that large bulky ligands can slow down the reaction course substantially, switching to the alternative dissociative

mechanism is not likely in these cases.[34] Because of presence of the water molecule in reactants of eq. 1, the forward reaction can be regarded as a kinetic reaction of a pseudo-first order. Nevertheless, the backward reaction follows the second order kinetic formalism. Experimentally determined rate constants for dechlorination were published by Arpalahti et al.[26,27] for the first and second steps and both cis- and trans-conformers at T = 318.2 K and pH 2.8−3.4 and in a 0.1 M $NaClO_4$ solution.

Similarly, the rate constants for cisplatin interactions with guanine were estimated. In these studies either water replacement by the base (k_{P1} a k_{P2}) or hydration process of the already coordinated cisplatin with guanine (k_3) were considered:

$$cis-[Pt(NH_3)_2ClN7(G)]^+ + H_2O \xrightarrow{k_3} Cl^- + cis-[Pt(NH_3)_2(H_2O)N7(G)]^{2+}$$

$$cis-[Pt(NH_3)_2Cl(H_2O)]^+ + G \xrightarrow{k_{P1}} H_2O + cis-[Pt(NH_3)_2ClN7(G)]^+$$

$$cis-[Pt(NH_3)_2(H_2O)_2]^{2+} + G \xrightarrow{k_{P2}} H_2O + cis-[Pt(NH_3)_2(H_2O)N7(G)]^{2+} \quad (3)$$

Based on several studies,[29,35-41] it is also possible to determine the rate constants of the reactions in eq. 3: $k_3 = 7.6\text{x}10^{-5}$ [s^{-1}], $k_{P1} = 1.5\text{x}10^{-4}$, and $k_{P2} = 92$ [$M^{-1}s^{-1}$] (averaging the cisplatin concentration by about 5 μM and the guanine concentration by about 0.8 mM for both subsequent reactions). Note that the value of the k_3 rate constant is comparable with values k_1 and k_2 of the reactions from eq. 1 and Table 7 (cf. below). Also, based on the values of k_{P1} and k_{P2} , it is obvious that guanine interacts substantially faster with the diaqua Pt-complex (by about 5 orders of magnitude). The experimental data unambiguously reveal the important difference between the activation processes in the first and second step.

Despite the question whether the equilibrium for the hydration process can occur, there is a factor which facilitates the reaction course, namely the decreased concentration of Cl^- anions during cisplatin passage from blood (with [Cl^-] about 100 mM) to a cellular environment (with [Cl^-] about 10-80 mM). The chloride concentration further drops down in the cellular nucleus to a value about 4 mM. This forces higher yields of the hydration products, according to LeChatelier-Braun-van Hoff's principle.

3. Quantum Chemical Calculations Related to Cisplatin Studies

One of the first researchers who applied the theoretical approaches to study cisplatin was Lipinski.[42] In his pioneering work, many important aspects of cisplatin behavior were investigated using a semiempirical approach. This includes hydration, cisplatin dimerization, and bonding to phosphate and guanine. The first ab initio calculations of cisplatin complexes with DNA bases were performed by Basch et al.[43] who also introduced the relativistic pseudopotentials for the platinum atom. The calculated coordination energies were already very accurate (e.g., bond dissociation energy (BDE) of the Pt-N7(guanine) dative bond was estimated to be approximately 114 kcal/mol). In 1990 Kozelka and coworkers carried out classical molecular mechanics calculations on the cisplatin-DNA oligomeric sequence.[44-46] Further, they recently reported explicit-solvent nanosecond-scale molecular dynamics simulation of a platinated DNA duplex.[47] Since the empirical parameters for platinum were not available, they fitted the results of ab initio Hartree-Fock obtained in a minimal basis set. Despite the very approximate estimation of the empirical force field parameters, they were able to predict the experimental measurements with very good accuracy.

Individual conformers of cis/transDDP were investigated by Pavankumar et al.[48] combining the the second order Møller-Plesset perturbation theory (MP2) approximation with several basis sets for the determination of the bonding properties, vibrational frequencies, and charge densities. Similar work was performed by Carloni and coworkers[49,50] using DFT techniques for the gas-phase and solid state calculations. They also performed a comparative study of the properties of cisplatin and carboplatin.[51] Different functionals were utilized for the determination of the molecular structure and vibrational spectra of carboplatin and cisplatin,[52] and the calculated spectroscopic data were compared for both platinum complexes with experimental measurements. The transition states for the chloride ligand replacement by water and guanine were studied by Chval et al.[53] The complex of cisplatin with 1,2-d(GpG) bases was examined by Carloni and coworkers.[54] In this study some hydration aspects of cisplatin were predicted using Car-Parrinello MD simulations.

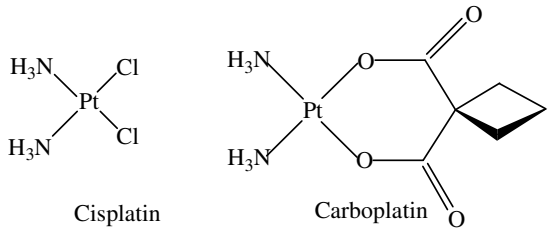

Cisplatin Carboplatin

Competitive effects for the interactions of cisplatin with various active sites in the cellular environment are discussed in papers of Deubel.[55,56] In the earlier paper, energetic and structural data of complexes with the different substituted ligands were explored. The more recent work deals with kinetic factors in the relation to the transition state (TS) for water replacement of the semihydrated cisplatin complex (cis-$[Pt(NH_3)_2(H_2O)Cl]^+$) with either an N- or S-containing ligand (thiopheneimidazol, dimethyl sulphide, or methanethiolate which serve as amino acid models). Deubel concluded the kinetic preference of N-sites over S-nucleophiles where the important role is played by the electrostatic terms. In addition, the aliphatic/aromatic character of the substituent as well as the influence of different dielectric constants of the environment are very important. A more realistic model for the aqua-ligand replacement with adenine and guanine was studied in works of Chval et al.[53,57] and Eriksson and coworkers.[58] They performed independently the estimation of the thermodynamic and kinetic parameters of this process.

The coordination of cisplatin to DNA purine bases represents a frequent topic of many recent papers. A study on the comparison of the cisplatin and cispalladium interaction with guanine was published by the Leszczynski group.[59] In addition, a possible chelation of cisplatin to the O6 and N7 guanine sites was explored. They showed that the possible deformations of Pt-adducts with a GC base pair can be stabilized in the case of an isolated pair resulting in the alteration of the (non-planar) H-bonding pattern. The Car-Parrinello/Molecular Dynamics (CPMD) study of cisplatin bound to DNA oligomer models was performed by Spiegel et al.[60] where besides the structural and energetical parameters, NMR shifts of the ^{195}Pt nucleus were also observed. Large fluctuation of these shifts during the dynamical simulations was reported.

Comprehensive computational studies of cisplatin compounds were performed by the Lippard group. In one of their works the strength of the N-glycosyl bonds after platination was investigated. It was shown that, while

protonation of the N7 position of guanine accelerates the depurination reaction, the cisplatin adduct does not change the glycosyl bond substantially.[61] They also explored the character of Pt-X bonds (X=Cl, O, N, and C) for various ligands: Cl, H_2O, NH_3, CO, and guanine.[62] The decreased strength of the C-O bond (in carbon-oxide containing ligands) was demonstrated with a decreasing total charge of platinum complexes. The question of guanine preference over adenine was examined in another work.[61] The same study also addressed the existence of the TS structure and the role of kinetic aspects on the preference of guanine adducts. The conclusion about the estimation of activation barriers are in very good accord with previously mentioned studies of Chval et al.[57] and Eriksson and coworkers.[58] The thermodynamic results can be compared with similar results from our group[63,64] where cisplatin bridges were examined between purine bases together with the influence of the sugar-phosphate backbone on the Pt-N7 bonds. Mispairs in DNA caused by different stabilizations of rare tautomers after platination of the N4-cytosine and N6-adenine sites were explored by Šponer et al.,[65] and a similar study was conducted for the N7-guanine and adenine sites by Burda et al.[66,67] Possible point mutations could occur in the case of adenine and cytosine where the imino-tautomer is more preferable over regular N6 and N4 amino forms under amino-platination. Interestingly, it was argued that the amino-platination promotes the tautomerism via substantial changes of the electronic structure of bases; therefore, the effect remains fully expressed under polar solvent conditions. A similar effect was also revealed for mercury and may be a common source of mutations in DNA upon metal binding. In contrast, the tautomers obtained by the N7 metalation are stabilized essentially by the electrostatic effects, and the formation of these tautomers is thus expected to be inhibited to a large extent by polar solvents. A similar conclusion was derived for the adenine protonation upon platinum binding to ring nitrogen atoms.[68] While the gas phase calculations show that the adenine proton affinity is dominated by the formal charge of the metal adduct, the corresponding solution pK_a values are independent of the charge of the metal in a wide range of −1 to +3. The platination nevertheless shifts the adenine pK_a due to nonelectrostatic effects. These nonelectrostatic effects are also seen in the gas phase QM calculations, albeit being much weaker compared to the electrostatics that dominate in the gas phase. Another recent study (combination of experimental and computational approaches) revealed that platination can cause cytosine deamination which also is a possible source of

mutations in DNA under metal binding.[69] The effect of platination on Watson-Crick base pair interactions was explored,[67] and the study clearly shows that the G-C base pair strength is increased via polarization effects.

4. The Topics of the Review

There are several questions which will be addressed within this review.

- The thermodynamic surface for the hydration of square-planar platinum(II) will be explored, and general conclusions on the solvation will be drawn.
- A comparison of the thermodynamical hydration surfaces of platinum and palladium complexes will be done showing that the SAR (structure and activity relationship) is not valid in relation to the cisplatin anticancer activity.
- Closer insight to the detailed molecular mechanism of the cisplatin ligand replacement can be used for the determination of both the thermodynamic and kinetic parameters from the Eyring TST theory.
- The influence of the surrounding environment will be examined in the last part revealing the key role of the proper screening of electrostatic interactions for accurate prediction of physico-chemical behavior of the systems under study.

5. Calculations of Platinum(II) Hydration Surface

5.1 Computational Model

A very accurate computational methodology based on MP4 single-point energy calculations was chosen for the evaluation of the selected hydration schemes. The methodology is based on the Gaussian theory ideas[70] that were modified for the determination of the total energies of all involved platinum complexes. The necessary modifications for the inclusion of the pseudopotentials were indicated so that the following "recipe" could be suggested:

- The most stable rotamers for all investigated species were found at the MP2/6-31G(d) level using the frozen-core approximation. The MWB-60

energy-averaged pseudopotentials from the Stuttgart/Dresden laboratory[71] were used for a description of the Pt atom. The 5s and 5p electrons of Pt were also kept in the frozen core at this step. The suggested basis set was extended with one set of f functions. Their exponent (α_f = 0.9804) was obtained by minimizing the ground state energy of the Pt atom at the CCSD level. The global minima of the considered complexes were further reoptimized at the MP2(full) level.

- Zero-point vibration energies (ZPVE) were determined at the HF level with the same basis set after another reoptimization at this level.
- Spin-orbit (SO) coupling corrections were calculated for the Pt atom since the relativistic effects are essential for species containing heavy elements. Other scalar relativistic corrections like the Darwin and mass-velocity terms are supposed to be implicitly included in (quasi)relativistic pseudopotentials because they mostly affect the core region of the considered heavy element. Their secondary influence can be seen in the contraction of the outer s-orbitals and the expansion of the d-orbitals. This is considered in the construction of the pseudoorbitals. The effective SO operator can be written within pseudopotential (PS) treatment in the form[71-75]

$V_{SO}^{(\lambda)}(i) = \sum_{l=1}^{l_{\max}} \frac{2\Delta V_{SO}^{(\lambda)}(r_{i\lambda})}{2l+1} P_l^{(\lambda)} \boldsymbol{l}_i . \boldsymbol{s}_i P_l^{(\lambda)}$, where $\boldsymbol{l}_i$ and $\boldsymbol{s}_i$ are corresponding momentum operators of the *i*th electron, and λ labels the atomic core described with the pseudopotentials. $P_l^{(\lambda)}$ is the projection operator: $P_l^{(\lambda)} = \sum_{m=-l}^{l} \left| Y_{lm}^{(\lambda)} \right\rangle \left\langle Y_{lm}^{(\lambda)} \right|$. The radial parts of the pseudopotentials are fitted in terms of Gaussian functions: $\Delta V_{SO}^{(\lambda)}(r_{i\lambda}) = \sum_k \Delta B_{ik}^{(\lambda)} \exp(-\beta_{ik}^{(\lambda)} r_{i\lambda}^2)$.

In our previous work[76] the Pitzer's version[77-79] of the COLUMBUS program[80] was used. Here, an implementation of the SO coupling in the MOLPRO program suite[81] was employed. For the SO interaction energies, averaged CAS wave functions were used with 6 singlet and 10 triplet reference states. With these numbers, the order of atomic spectrum lines (the ^{3}D, ^{3}F, ^{1}D and ^{1}S states) was successfully reproduced. The three highest occupied and three lowest unoccupied orbitals were chosen as the active space. Some preliminary calculations demonstrated that the results are not too sensitive to the size of the active space. A larger space (e.g., 4+4 or more) would be substantially more time demanding with practically the same

effect on the SO coupling energies. To the contrary, it was of crucial importance to keep the number of states treated in the averaged CAS calculation and in the following CI-SO procedure as large as possible. A smaller number of states (5 triplet and 6 singlet states) did not reproduce the calculated spectrum of the Pt atom even qualitatively.[82]

- The inclusion of higher components of the correlation energy (not included in up to the fourth order of perturbation theory, MP4) was performed with the CCSD(T) method. This method is known to be very reliable for systems containing transition metals, while some similar approaches like QCISD(T) failed.[83,84]
- The role of increased size of basis sets was examined in two sets of calculations:

a) with another set of diffuse functions (the MP4/6-31+G(d)) calculations, where the original set of the Pt atom pseudo-orbitals was also augmented with s-, p-, and d-functions ($\alpha_s = 0.0075$, $\alpha_p = 0.013$, and $\alpha_d = 0.025$) for the sake of consistency.

b) with extension by polarization functions (computed at the MP4/6-31G(2df,p) level); for the Pt atom a set of the f-functions was replaced by a new set of 2fg AOs ($\alpha_f = 1.4193$, 0.4662, and $\alpha_g = 1.2077$) optimized for the Pt ground state with the CCSD method.

c) the last basis set extension resulted in calculations at the MP2(full)/aug-cc-pvtz level. A new contraction scheme was used for the platinum atom (8s,7p,6d)/[6s,5p,4d] where the three outermost d-primitive gaussian functions were excluded from contraction. This basis set was augmented with the diffuse functions mentioned above and with a set of 3f, 2g polarization functions ($\alpha_f = 1.8466$, 0.8065, 0.2937, $\alpha_g = 2.0049$, 0.7040) (optimized for the Pt ground state).

- Utilizing the PS treatment, some portion of the correlation energy corresponding to inclusion of the inner Pt electrons was lost in the MP2(full) calculations. Therefore, at least part of this lost energy can be estimated in the so-called core-polarization potentials (CPP) which were used for the estimation of the core-valence electron interactions as originally suggested by Preuss[85] and Müller.[86] The effective core-polarization potentials can be written in the form $V_{CPP} = -\frac{1}{2}\sum_c \alpha_c . f_c . f_c$, where f_c is the electric field vector of electrons and the other core shells which act on a given core shell

$\underline{c}$: $f_c = \sum_i \frac{r_{ic}}{r_{ic}^3}.C(r_{ic},\rho_c) - \sum_{c'\neq c} \frac{R_{c'c}}{R_{c'c}^3} Z_{c'}$, with $r_{ic} = r_i - r_c$, and $R_{c'c} = R_{c'} - R_c$.

The expression $C(r_{ic},\rho_c)$ represents a so-called cutoff function. This function was introduced mainly as a short-range correction of the core effects. [86] In this form of CPP, there are two explicit variables, a core polarizability α_c and a parameter ρ_c in the cutoff function of the potential. The core polarizability was estimated from a calculation on the Pt^{18+} ion at the non-relativistic HF level. For this purpose the Huzinaga well-tempered uncontracted basis set[87,88] was used. The set of 5g functions with exponents, taken from the most diffuse f-functions, was added for better flexibility. The polarizability was calculated using analytical derivatives with the Gaussian 98 program package. The value obtained is $\alpha(Pt^{18+}) = 0.1297$ Å.^{3} The polarizability obtained in this way can serve as a rough estimate only. The other variable parameter ρ in the cutoff function for the short range potential $C(r_{ic},\rho_c) = (1 - e^{(r_{ic}/\rho_c)^2})$ was in the original work[86] adjusted to the ionization potential (IP). However in the case of small-core pseudopotentials, the IPs are not so sensitive to the change of the cutoff parameter. Thus, another quantity had to be investigated for this purpose. We have found that the eigenvalue of the electrons in the 5s AO could be considered, and the cutoff parameter was adjusted so that the orbital energy of the 5s fits the corresponding value obtained from the Dirac-Fock equations published by Desclaux.[89] In this way the ρ = 1.245 value was achieved.

The final ***ΔE$_0$(G3)*** energies at 0K can be evaluated according to:

$$\Delta E_0(G3) = \Delta E(combined) + E(ZPVE)$$

with *ΔE(combined)* defined as:

$$\Delta E(combined) = E[MP4/6-31G(d)] + \Delta E(+) + \Delta E(2df,p) + \Delta E(CC) + \Delta E(CPP) + \Delta E(G3large) + \Delta E(SO)$$

where individual terms come from the following equations:

$$\Delta E(CC) = E[CCSD(T)/6-31G(d)] - E[MP4/6-31G(d)]$$

$$\Delta E(+) = E[MP4/6-31+G(d)] - E[MP4/6-31G(d)]$$

$$\Delta E(2df) = E[MP4/6-31G(2df,p)] - E[MP4/6-31G(d)]$$

$$\Delta E(G3large) = E[MP2(full)/aug-cc-pvtz] - E[MP2/6-31G(2df,p)] - E[MP2/6-31+G(d)] + E[MP2/6-31G(d)]$$

$$\Delta E(CPP) = E[MP4/CPP+6-31G(d)] - E[MP4/6-31G(d)]$$

All studied complexes were considered in a square-planar arrangement. The electronic ground state of such platinum complexes is close-shell singlet.

The main focus of the investigations is a comparison of cis- and transplatin. Nevertheless the charged complexes $Pt(NH_3)_4^{2+}$ and $PtCl_4^{2-}$ were also considered under the reaction (hydration):

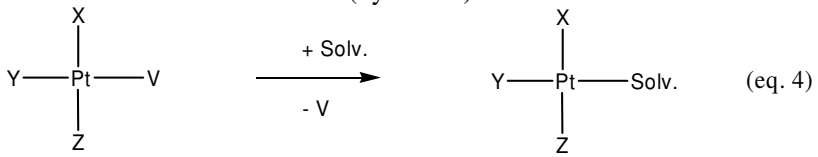

(eq. 4)

All of the reactions where chloride or the NH_3 group was replaced with either H_2O and OH^- were examined. This should, to a certain amount, reflect processes with both a constant and a varied pH of the solution.

5.2 Optimized Structures of Square-Planar Platinum Complexes

The most stable rotamers were found for the considered complexes. The individual Pt-L bond distances (L = heavy atom of the ligand) are collected in Table 1. In accordance with Pavankumar et al.,[48] it was found the C_{2v} conformer is the global minimum for the cisplatin complex. For the trans-DDP complex, the expected candidate for the global minimum was rotamer with C_{2h} point group symmetry (with axes perpendicular to ligand plane, cf. Figure 2). However, another structure with C_{2v} symmetry (axes colinear with Cl-Pt-Cl bonds) was found to be slightly lower in energy (0.5 kJ/mol). This conclusion was also verified with the additional set of optimizations where larger basis set was employed - at the MP2(FC)/aug-cc-pvtz level. This interesting finding should not be overemphasized since internal molecular movement can easily cover such a difference at higher temperature.

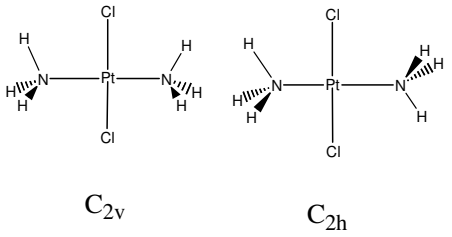

C_{2v} C_{2h}

Figure 2. A comparison of the C_{2h} and C_{2v} geometries of the trans-DDP complex.

Table 1. Pt-ligand distances (in Å) obtained at the MP2/6-31G(d) optimization level.

Geometry	Pt – N	Pt- Cl	Pt – O[a]
$[Pt(NH_3)_4]^{2+}$	2.055	-	-
$[Pt(NH_3)_3(H_2O)]^{2+}$	2.045/2.057/2.012	-	2.077
$[Pt(NH_3)_3(OH)]^{+}$	2.035/2.098/2.035	-	1.950
cis-$Pt(NH_3)_2Cl_2$	2.056	2.275	-
cis-$[PtCl(NH_3)_2(H_2O)]^{+}$	2.068/2.002	2.254	2.078
cis-$PtCl(NH_3)_2(OH)$	2.040/2.081	2.283	1.953
cis-$[Pt(NH_3)_2(H_2O)_2]^{2+}$	2.004	-	2.081
cis-$[Pt(NH_3)_2(H_2O)(OH)]^{+}$	2.092/1.996	-	2.074/1.944
cis-$Pt(NH_3)_2(OH)_2$	2.130	-	1.967
cis-$PtCl_2(NH_3)(H_2O)$	2.044	2.239/2.273	2.123
cis-$[PtCl_2(NH_3)(OH)]^{-}$	2.016	2.351/2.301	1.977
cis-$PtCl_2(H_2O)_2$	-	2.238	2.109
cis-$[PtCl_2(H_2O)(OH)]^{-}$	-	2.324/2.256	2.112/1.989
cis-$[PtCl_2(OH)_2]^{2-}$	-	2.372/2.406	1.997/1.980
cis-$PtCl(NH_3)(H_2O)(OH)$	2.067	2.248	2.106/1.955
cis-$[PtCl(NH_3)(OH)_2]^{-}$	2.047	2.358	1.971/1.973
trans-$Pt(NH_3)_2Cl_2$	2.025	2.293	-
trans-$[PtCl(NH_3)_2(H_2O)]^{+}$	2.030/2.045	2.228	2.12
trans-$PtCl(NH_3)_2(OH)$	2.019	2.320	1.979
trans-$[Pt(NH_3)_2(H_2O)_2]^{2+}$	2.049	-	2.033
trans-$[Pt(NH_3)_2(H_2O)(OH)]^{+}$	2.031/2.038	-	2.148/1.927
trans-$Pt(NH_3)_2(OH)_2$	2.014	-	1.999
trans-$PtCl_2(NH_3)(H_2O)$	1.984	2.290	2.070
trans-$[PtCl_2(NH_3)(OH)]^{-}$	2.06892	2.315/2.312	1.960
trans-$PtCl_2(H_2O)_2$	-	2.289	2.024
trans-$[PtCl_2(H_2O)(OH)]^{-}$	-	2.301/2.326	2.177/1.935
trans-$[PtCl_2(OH)_2]^{2-}$	-	2.338/2.337	2.026/2.026
trans-$[PtCl(NH_3)(OH)_2]^{-}$	2.003	2.310	2.010/2.007
$[PtCl_3(H_2O)]^{-}$	-	2.248/2.306/2.306	2.117
$[PtCl_3(OH)]^{2-}$	-	2.346/2.385/2.320	1.987
$[PtCl_4]^{2-}$	-	2.329	-

[a]in mixed complexes the Pt-O bonds longer than 2.0 Å belong to H_2O, others to OH^-.

In addition, the application of different computational techniques could possibly change the preference. The schematic pictures of the global minima

for the most important compounds of the reaction path are demonstrated in Figure 3.

Following the suggested Gaussian theory, all systems were reoptimized at the MP2 level without any frozen core orbitals.

The shortest Pt-bonding distances were found for negatively charged OH^- ligands (on average about 1.96 Å). Ammonia and water coordinations are similar; the average Pt-N distance is about 2.04 Å and Pt-O about 2.10 Å.

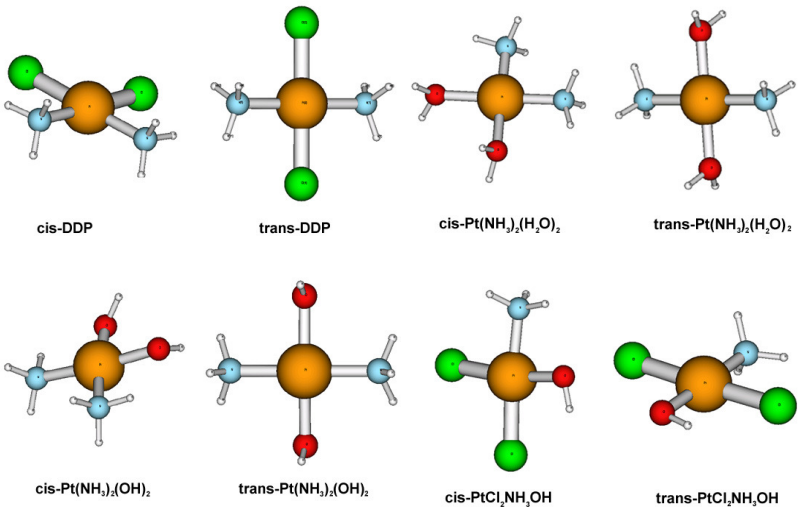

Figure 3. Schematic pictures of some of the important global minima structures on the hydration energy surface.

The longest bonds are the Pt-Cl bonds. All the Pt-ligand distances exhibit relatively large fluctuation, for example, in the Pt-Cl bond they vary from 2.23 Å (in positively charged particle $[trans\text{-}Pt(NH_3)_2Cl(H_2O)]^+$) to 2.35 Å (in negatively charged $[cis\text{-}Pt(NH_3)Cl_2(OH)]^-$ species). The total charge of the complex influences the bond length; the longer bonds in negatively charged complexes reflect the larger contribution of the electron repulsion. All Pt complexes basically preserve the square planar arrangement, one of the largest deviations of the dihedral angle from the plane being 8° in the case of the trans-Pt $(NH_3)_2(OH)_2$ complex. Bond angles also remain close to 90°; the smallest bond angle is ∠ N-Pt-O = 82° in the negatively charged cis-$Pt(NH_3)Cl_2(OH)$ complex.

5.3 The Analysis of the Terms in the ΔE_0 (G3) Evaluation

In the applied methodology, various corrections are added to the MP2(full)/6-31G(d) level, assuming that these contributions are basically additive. Table 2 contains the individual contributions of the examined corrections. It can be seen that an increase of the order of PT leads to lower total energies by about 30 kcal/mol (column labeled ΔE(MP4)). The column ΔE(CC) sums all the contributions from the single and double excitations together with the non-iterative triple contributions, according to the CCSD(T) theory. These contributions are very close to the MP4-SDTQ results; the differences are not larger than a few kcal/mol. Comparing the MP4-SDQ correlation energy with the corresponding CCSD energy, the values obtained within PT are generally smaller for positively charged complexes and larger for neutral and negatively charges species. Energy contributions of triples are systematically lower in the case of the CCSD(T) method (up to 2 kcal/mol). Hence, for positively charged systems, these two trends (larger triples contributions and smaller SDQ values) compensate at the MP4 level. In the case of 2+ charged complexes, the final CCSD(T) energies are smaller than the corresponding MP4 energies.

The next columns of Table 2 display the role of larger basis sets augmented by the polarization and diffuse functions. Here it can be noticed that the polarization functions are more important than the inclusion of the diffuse functions. The only exception can be noticed in the presence of the OH^- ion which seems to be fairly sensitive to the additional diffuse functions. In these cases the additional set of diffuse functions gives improvement of about 12kcal/mol in comparison, for example, with complexes with water. Such a trend is easy to understand because diffuse functions are more important for the description of the loosely bonded electrons in negatively charged systems.

The column (ΔE(MP2/G3)) contains the differences between the MP2(full) energies with a basis set of augmented-triple-zeta quality and the 6-31G(d) basis set. The size of these numbers clearly demonstrates the fact that the split-valence double-zeta basis sets are far from being complete.

The ZPVE contributions closely reflect the number of bonded hydrogens because the vibrations of the light elements can more easily absorb energy and thus represent the most important contribution to the final ZPVE.

Table 2. Main energy contributions for the evaluation of the ΔE_o(G3) energies of the Pt(II) complexes (in a.u.).

Complex	E(MP2)[a]	ΔE(MP4)[b]	ΔE(CC)[c]	ΔE(2df)[d]	ΔE(+)[d]	ΔE(MP/G3)[e]	ZPVE	ΔE(SO)	ΔE_o(G3)
$[Pt(NH_3)_4]^{2+}$	-343.8775	-0.0617	-0.0009	-0.3131	-0.0108	-0.7158	0.1742	-0.0035	-344.8286
$[Pt(NH_3)_3(H_2O)]^{2+}$	-363.6839	-0.0565	-0.0006	-0.3226	-0.0132	-0.7379	0.1590	-0.0038	-364.6535
$[Pt(NH_3)_3(OH)]^{+}$	-363.4588	-0.0554	0.0026	-0.3190	-0.0169	-0.7392	0.1454	-0.0056	-364.4291
cis-$Pt(NH_3)_2Cl_2$	-1150.9442	-0.0597	0.0014	-0.3266	-0.0141	-0.7933	0.0895	-0.0056	-1151.9818
cis-$[PtCl(NH_3)_2(H_2O)]^{+}$	-767.2959	-0.0556	0.0006	-0.3296	-0.0156	-0.7761	0.1173	-0.0059	-768.3116
cis-$PtCl(NH_3)_2(OH)$	-766.9184	-0.0546	0.0037	-0.3244	-0.0193	-0.7769	0.1034	-0.0019	-767.9217
cis-$[Pt(NH_3)_2(H_2O)_2]^{2+}$	-383.4902	-0.0512	-0.0002	-0.3323	-0.0151	-0.7596	0.1441	-0.0067	-384.4829
cis-$[Pt(NH_3)_2(H_2O)(OH)]^{+}$	-383.2696	-0.0505	0.0028	-0.3284	-0.0298	-0.7602	0.1307	-0.0060	-384.2579
cis-$Pt(NH_3)_2(OH)_2$	-382.8832	-0.0494	0.0057	-0.3233	-0.0307	-0.7629	0.1166	-0.0046	-383.8673
cis-$PtCl_2(NH_3)(H_2O)$	-1170.7617	-0.0551	0.0015	-0.3356	-0.0143	-0.8126	0.0748	-0.0068	-1171.8175
cis-$[PtCl_2(NH_3)(OH)]^{-}$	-1170.2449	-0.0537	0.0038	-0.3268	-0.0243	-0.8111	0.0609	-0.0068	-1171.2958
cis-$PtCl_2(H_2O)_2$	-1190.5754	-0.0507	0.0017	-0.3463	-0.0181	-0.8353	0.0600	-0.0055	-1191.6476
cis-$[PtCl_2(H_2O)(OH)]^{-}$	-1190.0618	-0.0493	0.0036	-0.3372	-0.0258	-0.8320	0.0460	-0.0081	-1191.1333
cis-$[PtCl_2(OH)_2]^{2-}$	-1189.3844	-0.0489	0.0060	-0.3275	-0.0375	-0.8333	0.0322	-0.0069	-1190.4522
cis-$PtCl(NH_3)(H_2O)(OH)$	-786.7362	-0.0499	0.0036	-0.3340	-0.0202	-0.7976	0.0885	-0.0059	-787.7639
trans-$Pt(NH_3)_2Cl_2$	-1150.9652	-0.0590	0.0010	-0.3275	-0.0150	-0.7934	0.0900	-0.0060	-1152.0034
trans-$[PtCl(NH_3)_2(H_2O)]^{+}$	-767.2966	-0.0557	0.0006	-0.3301	-0.0149	-0.7772	0.1170	-0.0061	-768.3125
trans-$PtCl(NH_3)_2(OH)$	-766.9279	-0.0539	0.0031	-0.3236	-0.0196	-0.7759	0.1032	-0.0061	-767.9384
trans-$Pt(NH_3)_2(OH)_2$	-382.8840	-0.0435	0.0051	-0.3280	-0.0256	-0.7627	0.1162	-0.0060	-383.8758
trans-$PtCl_2(NH_3)(H_2O)$	-1170.7732	-0.0544	0.0011	-0.3380	-0.0177	-0.8154	0.0752	-0.0060	-1171.8300
trans-$[PtCl_2(NH_3)(OH)]^{-}$	-1170.2405	-0.0544	0.0038	-0.3312	-0.0243	-0.8154	0.0609	-0.0043	-1171.2912

Table 2. Main energy contributions for the evaluation of the ΔE_o(G3) energies of the Pt(II) complexes (in a.u.) (cont.).

Complex	E(MP2)[a]	ΔE(MP4)[b]	ΔE(CC)[c]	ΔE(2df)[d]	ΔE(+)[d]	ΔE(MP/G3)[e]	ZPVE	ΔE(SO)	ΔE_o(G3)
trans-$PtCl_2(H_2O)_2$	-1190.5743	-0.0504	0.0011	-0.3482	-0.0199	-0.8372	0.0603	-0.0049	-1191.6479
trans-$[PtCl_2(H_2O)(OH)]^-$	-1190.0614	-0.0500	0.0042	-0.3405	-0.0252	-0.8350	0.0462	-0.0051	-1191.1298
trans-$[PtCl_2(OH)_2]^{2-}$	-1189.3759	-0.0489	0.0052	-0.3315	-0.0395	-0.8392	0.0320	-0.0065	-1190.4494
tr-$PtCl(NH_3)(H_2O)(OH)$	-786.7398	-0.0491	0.0034	-0.3335	-0.0216	-0.7974	0.0887	-0.0061	-787.7681
$[PtCl_3(H_2O)]^-$	-1574.0964	-0.0547	0.0017	-0.3422	-0.0209	-0.8498	0.0323	-0.0083	-1575.1964
$[PtCl_3(OH)]^{2-}$	-1573.4315	-0.0542	0.0037	-0.3321	-0.0315	-0.8490	0.0185	-0.0084	-1574.5287
$[PtCl_4]^{2-}$	-1957.4764	-0.0589	0.0014	-0.3362	-0.0258	-0.8644	0.0046	-0.0098	-1958.6021

[a]optimized energy at the MP2(full)/6-31G* level.
[d]difference MP4 energies with larger basis sets.
[b]difference E(MP4)-E(MP2) (both with frozen core).
[e]difference E(MP2(full)/G3)-E(MP2(full)/6-31G*).
[c]difference E(CCSD(T))-E(MP4) with the 6-31G* basis set.

Very important also is the spin-orbit coupling. From Table 2, it can be seen that the heavier the complex, the larger the SO splitting. The negatively charged complexes also exhibit larger SO energies. Nevertheless these trends are only approximate since other effects are also important. From the calculated set, it is difficult to decide whether the cis- or trans-isomers could be more stabilized by the SO coupling.

5.4 Thermodynamical Surface for the Hydration of Pt(II) Complexes

The energetics for the designed hydration processes was determined using the ΔE_o (G3) values. Figure 4 displays the reaction energies schematically. In the fraction numbers, the numerator represents the energy of the cis-configuration and the denominator value of the trans-conformer.

In the left part of Figure 4 where the charged $[Pt(NH_3)_4]^{2+}$ complexes are displayed, the exchange of the first ammonia molecule with water proceeds with an endothermic step ($\Delta E = 20$ kcal/mol) if the total charge of the complex is preserved. This finding is in good accord with the generally known fact that transition metals prefer coordination with soft atoms like nitrogen or sulfur rather than the coordination with oxygen. Further hydration with the second water molecule requires a similar amount of energy. In the case of hydration with the OH^- ion, the positive charge of the complex is reduced, and a large amount of energy is released (more than 230 kcal/mol). Replacement with the second OH^- ion leads to a neutral complex releasing about 130 kcal/mol. Hence the final and most stable product of hydration of positively charged $[Pt(NH_3)_4]^{2+}$ is the neutral $Pt(NH_3)_2(OH)_2$ complex. This process is associated with a decrease in pH because two protons are the product of the hydration if the total charge is preserved. However, considerations of the role of pH is not simple since the $(NH_4)^+$ cations can be partially formed, reducing the concentration of the released protons.

In the right part of the scheme, the negatively charged $[PtCl_4]^{2-}$ complex is considered. Here, the substitution of the first chloride with water is about twice more exothermic than the substitution with the hydroxyl anion. Nevertheless the energies of the two reactions are relatively close. Water substitution becomes energetically more profitable only when diffuse functions are included in the basis set.

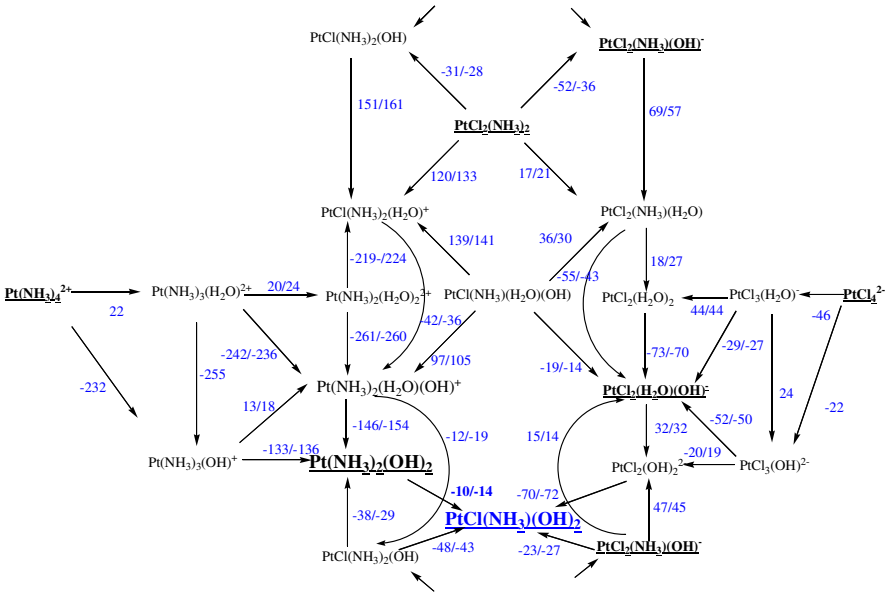

Figure 4. A complete reaction scheme up to two hydration particles. Numbers over reaction arrows represent the heats of reactions in kcal/mol. Fractions means reaction for cis-/trans-conformers, respectively.

The reason for the larger solvation energy can be seen in the higher stability of the singly charged $[PtCl_3(H_2O)]^-$ complex over the $[PtCl_3(OH)]^{2-}$ complex with two excess electrons. The second hydration step also favors a singly charged mixed water-hydroxyl complex ($[PtCl_2(H_2O)(OH)]^-$). This species represents the most stable complex on the reaction surface of $[PtCl_4]^{2-}$. Replacing the second chloride with a water molecule is a fairly endothermic step, and such complexes (neutral cis/trans-$PtCl_2(H_2O)_2$) lie remarkably higher than the charged $[PtCl_2(OH)_2]^{2-}$ species. Assuming that the $[PtCl_2(H_2O)(OH)]^-$ system is the final product of the $[PtCl_4]^{2-}$ solvation, the hydration process leads to a decrease in the pH since one proton from the dissociated water is released (and only partially compensated by HCl formation). In comparison with $[Pt(NH_3)_4]^{2+}$, the hydration process of $[PtCl_4]^{2-}$ is substantially less exothermic. Such a difference can be understood from the point of view of IPs and electron affinities (EA). Generally speaking, IP energies are much larger than EA energies for neutral molecules.

The hydration process of cis- and trans-DDP represents the most important case. The first step was found exothermic for substitution of both Cl^- and NH_3 ligands with the hydroxyl anion. A larger amount of energy is released when the ammine ligand is replaced, forming the negative $[PtCl_2(NH_3)(OH)]^-$ species. Subsequent deammination process of this complex is endothermic considering both water and the hydroxyl ion. Nevertheless dechlorination of this complex and replacement with a hydroxo-ligand leads to the release of more than 20 kcal/mol of energy. This mixed monoamine-monochloro-dihydroxoplatinum anion represents the global minimum of the whole hydration scheme. When the hydroxyl group is considered in the second solvation step of the $PtCl(NH_3)_2(OH)$ complex, the exothermic behavior is obtained for both dechlorination and deammination reactions. A smaller release of energy (slightly less than 30 kcal/mol) is connected with dechlorination, while more than 40 kcal/mol is gained in the NH_3 replacement reaction resulting in the global minimum structure. Thus, the interaction of cis- and transplatin with the water solvent provides the $[PtCl(NH_3)(OH)_2]^-$ anion as their most stable products followed by the neutral $Pt(NH_3)_2(OH)_2$ complex. These compounds represent the lowest lying complexes on the reaction surface. This conclusion is in partial agreement with experimental findings that cisplatin usually interacts with DNA bases in the hydrated form where two ammonia ligands are present.

Notice that within the suggested reactions, two protons dissociate, decreasing the pH of the solution.

The hydration of charged $[Pt(NH_3)_4]^{2+}$ leads to the $Pt(NH_3)_2(OH)_2$ complex. Neutral cis-/trans- DDP would thermodynamically prefer the $[PtCl(NH_3)(OH)_2]^-$ complex, which is slightly more stable. The cis-isomer can be considered as the global minimum on the generalized hydration surface. The position of a complex on this surface is determined as a sum of the total energies of the given complex and its ligand supplement. The ligand supplement for the complex contains the complete set of ligands (4x Cl^-, 4x NH_3, 2x H_2O, and 2x OH^-), omitting the ligands that are present in the given complex. This hydration energy surface for complexes from Figure 4 is drawn in Figure 5. As the reference energy, the value for the $[PtCl_4]^{2-}$ complex was set to zero, and the relative energies of the other complexes were determined. Figure 5 shows the positions of the complexes which have relative hydration energies lower than 50 kcal/mol. The most stable structures are the $[PtCl(NH_3)(OH)_2]^-$ anions with the trans isomer being approximately 2 kcal/mol above the cis isomer. The $Pt(NH_3)_2(OH)_2$ complexes are slightly more than 20 kcal/mol higher. In this case, the cis-$Pt(NH_3)_2(OH)_2$ isomer is about 5 kcal/mol above the trans isomer. Besides these very stable structures, other complexes were also found in their proximity: $[PtCl_2(NH_3)(OH)]^-$, cis-/trans-$[PtCl_2(H_2O)(OH)]^-$ which is slightly higher than the products of $[PtCl_4]^{2-}$ hydration, and the $PtCl(NH_3)_2(OH)$ complexes. Interestingly, the mixed $PtCl(NH_3)(H_2O)(OH)$ complexes lie lower than $PtCl_2(NH_3)_2$. It can be seen that among these complexes, there are three neutral structures and two negatively charged (1-) species for both cis and trans isomers. In these particular cases one or two ammine-ligands with a soft nitrogen (according to the HSAB principle[90]) are replaced with a harder oxygen, which has smaller affinity to platinum (and to transition metals in general). If such species are to be stable, additional forces must strengthen the dative bonds, which could be done by the additional electrostatic interactions $Pt^{\delta+}$ - $O^{\delta-}$ involving the negatively charged oxygen from the hydroxyl groups.

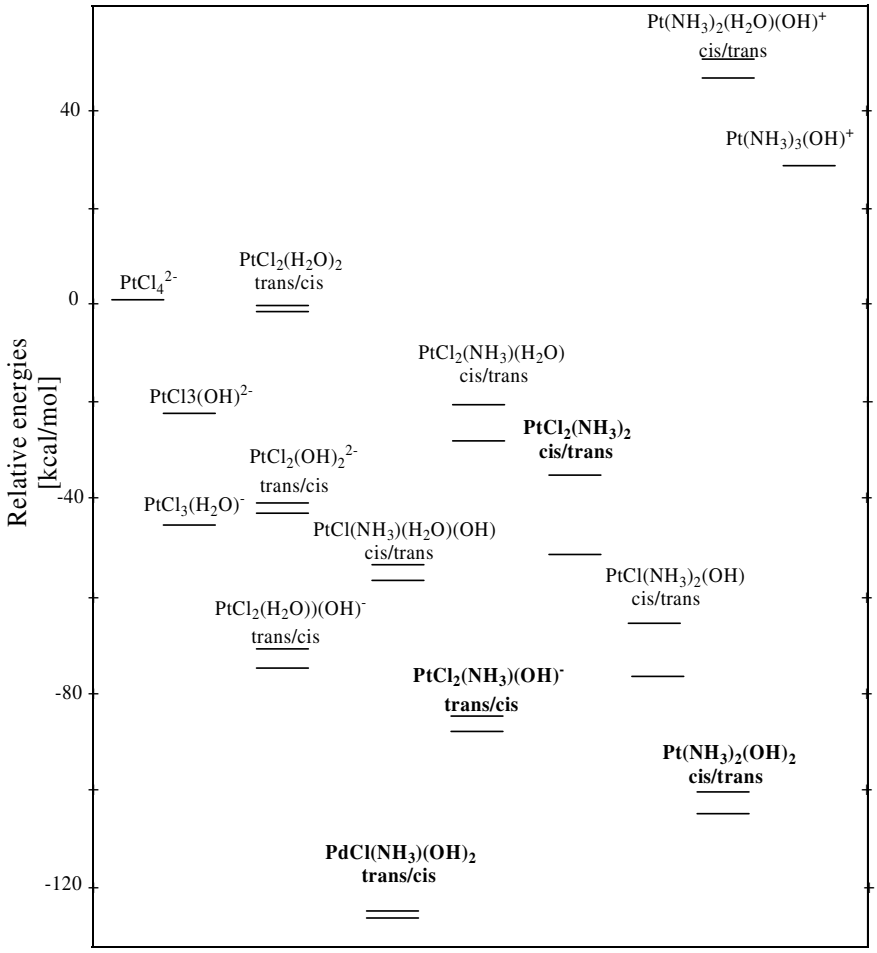

Figure 5. The generalized reaction surface for the chosen hydration scheme of the Pt(II) complexes. In the fraction, cis/trans under the chemical formula means that the cis isomer lies higher than the corresponding trans isomer. The complexes lying higher than 50 kcal/mol are not shown for the sake of lucidity.

6. Comparison of the Hydration Energy Surfaces of Pt(II) and Pd(II) Complexes

Palladium compounds have long been explored in relation to the possible interactions with DNA bases. In addition to numerous experimental work[91-93] a lot of theoretical papers have appeared due to the recent progress in computational quantum chemistry. Some of these studies provide the comparison of both structural and thermodynamical properties of palladium and platinum complexes. Generally, structural similarities are usually demonstrated.[9,10] As to other, for example, catalytic properties, the behavior of these two metals is not so similar. One of the reasons can be seen in the different electronic structure of the atoms. While Pd in the ground state favors state ^{1}S with a complete d-shell, the ground state of atomic Pt is ^{3}D where the 6s orbital is also partially occupied.[76] The DFT methods used for Pd(II) halide systems[94-96] show fairly good reliability. The BP86 functional (Becke's 88 exchange functional) was applied to the square planar palladium compound $[PdCl_4]^{2-}$. Recently an investigation of the solvation of square planar palladium complexes was published by Swang.[97] There, infrared and NMR spectroscopy results were compared with ab initio calculations at the Hartree-Fock level using MIDI basis set demonstrating relatively good agreement between the experimental and computational techniques.

It is well established that contrary to cisplatin, the analogous palladium compound is inactive as an anticancer drug.[98] It was observed experimentally that numerous analogous species with Pt(II) and Pd(II) have very similar structural parameters, but their kinetics are substantially different (ca. 10^4 times faster in the case of Pd(II) compounds).[9,10] The difference in the kinetics of the chemical reactions is important in understanding the various catalytic and biochemical roles of palladium- and platinum-based compounds.

For this purpose, the detailed energetics of the hydration processes for the selected square palladium complexes were examined using high-level quantum chemical calculations in order to compare the results with the corresponding energies of the platinum systems. The chosen methodology is based on the known role of individual contributions from Gaussian theory discussed above. The single-point calculations utilizing MP4(SDTQ) with the standard 6-31+G(d) Pople's basis set are sufficiently accurate. Analogous MWB-28 pseudopotentials were used for the description of Pd valence electrons, augmenting the suggested set of pseudo-orbitals with a set of

diffuse (α_s = 0.008, α_p = 0.012, and α_d = 0.03) and polarization (α_f = 1.47) functions for the sake of basis consistency.

6.1 Structures of the Palladium Complexes

The most important structural data are summarized in Table 3. The largest bond lengths are observed in the case of Pd-Cl bonds (about 2.31 Å). The Pd-O distances for aqua-ligands are about 2.10 Å, and the Pd-N bond lengths about 2.04 Å (note the analogous Pt-distances!). Some interesting exceptions can be seen, for example, in the $[Pd(NH_3)_3(OH)]^+$ complex where NH_3 in the trans position to the OH group has a relatively long Pd-N distance of 2.11 Å. The reason for such an extension stems from an induction effect which causes a shift in electron density towards the negatively charged OH group, resulting in a mild weakening of the Pd-N bond. The same effect is responsible for the prolongation of Pd-Cl bonds (up to 2.42 Å) in $[PdCl_y(OH)_x]^{2-}$ complexes. In the case of Pd-O bond lengths, the shortest bond lengths occur for the hydroxyl groups. Here, the influence of Coulombic forces leads to decreased Pd-O bond distances. Another interesting point is that the Pd-N distances are generally shorter than the Pd-O distances. This is the same feature as revealed for Pt(II) complexes, and generally it is not in accord with the covalent and/or atomic radii of nitrogen and oxygen. Both covalent and atomic radii are a little larger in the case of nitrogen. The observation can be explained by considering that the nitrogen atom belongs to the so-called soft (or borderline) atoms (ligands)[99,100] and that the oxygen atom belongs to hard atoms.[90]

A similar comparison of the interactions between magnesium and zinc-group cations with the nitrogen sites of DNA bases and water oxygen atoms can be found in one of our recent studies.[101] While in the case of the magnesium ion, the ratio of the Mg-O/Mg-N distances roughly follows the ratio of the O/N atomic radii. Zinc clearly favors interactions with nitrogen over oxygen; Zn-N distances are shorter than Zn-O.

Table 3. Bond lengths of individual Pd complexes (in Å) obtained at the MP2/6-31G(d) level of calculation.

Complex	Pd-N	Pd-Cl	Pd-O
$[Pd(NH_3)_4]^{2+}$	2.054	-	-
$[Pd(NH_3)_3(H_2O)]^{2+}$	2.042/2.016/2.054	-	2.083
$[Pd(NH_3)_3(OH)]^{+}$	2.044/2.110/2.044	-	1.925
cis-DDPd	2.070	2.254	-
cis-$[PdCl(NH_3)_2(H_2O)]^{+}$	2.008/2.076	2.229	2.082
cis-$PdCl(NH_3)_2(OH)$	2.099/2.060	2.271	1.925
cis-$[Pd(NH_3)_2(H_2O)_2]^{2+}$	2.004	-	2.083
cis-$[Pd(NH_3)_2(H_2O)(OH)]^{+}$	2.012/2.104	-	1.917/2.078
cis-$Pd(NH_3)_2(OH)_2$	2.080	-	1.946/1.946
cis-$PdCl_2(NH_3)(H_2O)$	2.056	2.250/2.223	2.133
cis-$[PdCl_2(NH_3)(OH)]^{-}$	2.031	2.345/2.293	1.952
cis-$PdCl_2(H_2O)_2$	-	2.223	2.115
cis-$[PdCl_2(H_2O)(OH)]^{-}$	-	2.257/2.322	1.953/2.127
cis-$[PdCl_2(OH)_2]^{2-}$	-	2.385/2.429	1.985/1.961
cis-$[PdCl(NH_3)(H_2O)_2]^{+}$	1.997	2.204	2.086/2.120
cis-$PdCl(NH_3)(H_2O)(OH)$	2.085	2.242	1.922/2.121
cis-$[PdCl(NH_3)(OH)_2]^{-}$	2.064	2.358	1.955/1.953
trans-DDPd	2.025	2.275/2.276	-
trans-$[PdCl(NH_3)_2(H_2O)]^{+}$	2.032/2.048	2.209	2.129
trans-$PdCl(NH_3)_2(OH)$	2.023	2.302	1.956
trans-$[Pd(NH_3)_2(H_2O)_2]^{2+}$	2.041	-	2.047
trans-$[Pd(NH_3)_2(H_2O)(OH)]^{+}$	2.049/2.038	-	1.906/2.155
trans-$Pd(NH_3)_2(OH)_2$	2.020/2.021	-	1.976/1.976
trans-$PdCl_2(NH_3)(H_2O)$	1.989	2.271/2.271	2.069
trans-$[PdCl_2(NH_3)(OH)]^{-}$	2.086	2.312/2.322	1.933
trans-$PdCl_2(H_2O)_2$	-	2.267/2.267	2.032
trans-$[PdCl_2(H_2O)(OH)]^{-}$	-	2.301/2.336	1.909/2.188
trans-$[PdCl_2(OH)_2]^{2-}$	-	2.36	2.001
trans-$[PdCl(NH_3)(H_2O)_2]^{+}$	2.067	2.226	2.045
trans-$PdCl(NH_3)(H_2O)(OH)$	1.985	2.307	1.942/2.087
trans-$[PdCl(NH_3)(OH)_2]^{-}$	2.019	2.31	1.984
$[PdCl_2(HCl)(H_2O)]$		2.215/2.213/2.433	2.150
$[PdCl_3(H_2O)]^{-}$	-	2.297/2.235/2.297	2.121
$[PdCl_3(OH)]^{2-}$	-	2.366/2.389/2.332	1.959
$[PdCl_4]^{2-}$	-	2.326	-

The obtained geometric parameters are in a good accord with the bond distances published in another study[97] where the Pd-O distances are 2.12 Å

for formic acid ligands and 2.01 Å for formate ligands. (These results were obtained at the Hartree-Fock level with a slightly smaller basis set.)

Recently a study of the excited states of cis/trans dichlorodiammineplatinum (DDP) and the palladium analogue has appeared.[102] The optimized geometries at the B3LYP/6-311G(3d,3p) level with Hay&Wadt ECP[103] (Pd-N and Pd-Cl distances are 2.20/2.10 Å and 2.31/2.36 Å for the cis/trans conformers, respectively) are in agreement with our results. All the bond lengths follow the trends found in experimental measurements: d(Pd-N) = 2.13/2.05 and d(Pd-Cl) = 2.26/2.33 Å (cis/trans).[104]

Comparing the corresponding platinum and palladium structures from Tables 1 and 3, it can be noticed the metal-ammine distances are very slightly (but still significantly) shorter in the case of Pd. On the contrary metal-chloride and more pronouncedly metal-oxygen (especially from hydroxo ligand) exhibit elongation in Pd-containing complexes. The average elongation is about 0.023 Å for Pd-OH bonds. This clearly points to some small differences in softness of both considered metals.[105-108]

6.2 Comparison of Pd(II) and Pt(II) Hydration Surfaces

The MP4 single-point calculations were performed for the optimized structures, and the hydration surface was evaluated according to equation 4. The individual reaction energies were used to compose an extended reaction scheme analogous to Figure 4. The discussion of the energies of individual reactions can follow the pattern of the corresponding Pt(II) complexes and, therefore, will be omitted.

The computational model used for the hydration of chosen platinum and palladium complexes allows a straightforward comparison of both hydration surfaces.

Figure 6 depicts a scheme with the differences between corresponding Pd and Pt reaction energies. For the sake of simplicity, a label Px was used for naming the metal atom in the complexes. Figure 6 underlines the striking extent of the similarity between the energetics of the both metals (in square planar coordination), at least for the hydration reactions presently investigated. The largest difference of the reaction energies is about 10 kcal/mol. This process is however irrelevant for metal hydration since it describes replacement of a chloride particle with an ammine-ligand in the formation of the cis-$[Px(NH_3)_2(H_2O)(OH)]^+$ complexes. Actually there are

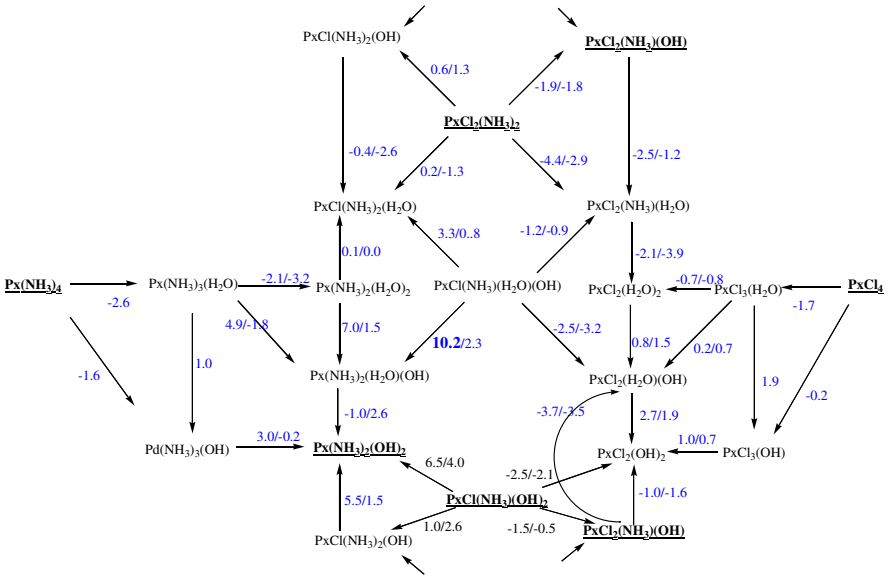

Figure 6. A differential hydration surface for the Pd(II) and Pt(II) complexes. The values are taken as a difference of the reaction energies E(Pd) – E(Pt) in kcal/mol.

only five reactions where the energy difference is larger than 4.5 kcal, and three of them contain this complex. The other two are related to a similar product of cis-$Px(NH_3)_2(OH)_2$. This is also in agreement with the fact that hydrated $Pd(NH_3)_2(OH)_2$ is slightly less stable. And consequently, the energy difference between the cis and trans conformer is also slightly increased.

In the other cases, there is not only qualitative but also quantitative agreement for all of the considered reactions. Regarding the markedly different biochemical roles of Pt- and Pd-based compounds, the very high degree of similarity between the calculated hydration surfaces of the Pd and Pt compounds does not correspond with the QSAR principle. The differences are considerably smaller compared to those we have recently noticed between Zn^{2+} and Mg^{2+} cations.[100,109] This clearly demonstrates that an understanding of the anticancer activity of the cisplatin complex is related not only to the thermodynamical description, but also some additional factors have to be included. This will be discussed in the next section.

7. Detailed Molecular Mechanism of the Hydration Processes of Platinum and Palladium Complexes

Deeper insight into the reaction mechanism of the hydration of cisplatin, transplatin, and their Pd-analogues is examined in this part. For such studies, the supermolecular approach was chosen where both reactants (metal complex with water) or both product molecules (metal complex with remoted ammonia or chloride particle) were treated as one system. This system was considered electroneutral and optimized using MP2 in singlet electronic groundstate. The most stable conformers of the reactants and products were selected for further analyses. For the determination of the transition state (TS) structures, an associative reaction mechanism was considered in accord with the studies of other authors.[33,34,53-55,60,110-113] For some difficult-to-optimize transition states, the QST3 algorithm of Schlegel was found to be very efficient.[114] Since frequency analysis was necessary for obtaining vibrational degrees of freedom, geometry re-optimizations of the global minima structures were carried out at the Hartree-Fock (HF) level followed by vibrational modes determinations. The 6-31+G(d) basis set was chosen for the first row elements. The chlorine, palladium, and platinum atoms were described by Stuttgart's relativistic energy-averaged pseudopotentials: Cl (MWB-10),[115] Pd (MWB-28),[116] and Pt (MWB-60)[71]

with consistent extensions of the polarization and diffuse functions, analogous to the methodology from the previous section. Lastly, single-point calculations were performed at the CCSD(T)/6-31++G(d,p) level.

The main aim of this section is to provide the detailed mechanism of the exchange reaction.

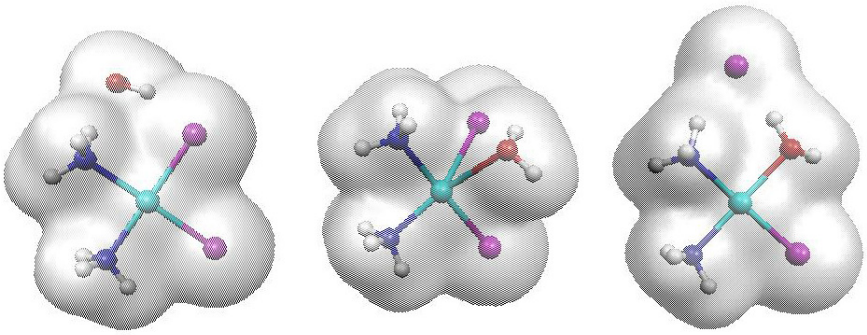

Figure 7. The supermolecular description of the reaction coordinate.

In the case of the second hydration step of cis-Px-X_2YW complexes, there are two possibilities how to replace one of the X ligands, yielding both cis-/trans-Px-XYWW' conformers (X, Y = Cl or NH_3 and W, W' = H_2O or OH). The solvent molecule can be placed in cis- or trans-coordination relative to the first solvent-ligand. Therefore three reactions are considered for these two cis-reactants.

The association energies between the two parts of the supermolecule were determined considering the basis set superposition error (BSSE)[117] of the Boys-Bernardi[118] counterpoise corrections.

Based on the known vibrational modes, as well as the energy and geometry characteristics of the studied reactions, the rate constants can be estimated according to Eyring's Transition State Theory (TST). The canonical rate constant for a bimolecular reaction at a given temperature proceeds according to the following equation:

$$k^{TST}(T) = \frac{kT}{h} . \frac{F^{TS}}{F^{M} F^{w}} . \exp(E_a / kT) \qquad (5)$$

where F^X are molecular partition functions per unit volume for TS, M-complex, and water; E_a is the activation energy. The rate constants were determined with the program DOIT (Dynamics Of Instanton Tunneling) obtained from Smerdachina et al.[119]

7.1 The Supermolecules and TS Structures

The reactants and products of hydration reactions are square planar complexes with one additional remote particle (water for reactants, and ammonium or chloride for products) in the vicinity of the Pt(II)-complex. Several positions of these molecules were examined for every system. Optimized interatomic distances between Pt and other heavy-atoms for the global minima are present in Table 4, and all examined reactions are drawn in Figure 8 where the used notation is also shown. The remote molecule is usually associated through two H-bonds, and the specific location of this molecule is controlled by the common rules valid for H-bonding. A relatively short Pt…O distance for the remote water (< 3.2 Å) in the cisDDP+H_2O supermolecule was found. Here, besides the two H_2N-H…O H-bonds, the additional weak interaction of HO-H…Pt can be noticed, which holds the water molecule above the Pt-complex plane.

Comparing the bond lengths of individual coordinated ligands, the remarkable influence of the trans-effect can be noticed. The ligand-strength diminishes as follows: hydroxyl group ≥ chloride >> ammonium > water. This relationship can be obtained from the comparison of many factors. For example, there are longer Pt-N and shorter Pt-Cl bonds in the cisplatin complex than in trans-DDP (where both chlorines compete with each other) or in cis- and trans-$PtCl_2(H_2O)_2$ complexes where a more pronounced reduction of the Pt-Cl bond distances occurs in the cis-conformer. The stronger trans effect of the hydroxyl group is evident from the previous sections where negatively charged complexes were also treated and a comparison of the $[PtCl_4]^{2-}$ and $[PtCl_3(OH)]^{2-}$ anions clearly supports the order.

Table 4. The bond distances of Px-X where Px=Pd or Pt, and X=N, O or Cl.

	Pt-N	Pt-N	Pt-Cl	Pt-Cl	Pt-O	Pt-O	Pd-N	Pd-N	Pd-Cl	Pd-Cl	Pd-O	Pd-O
R01	2.051	2.052	2.277	2.277	3.183		2.059	2.059	2.260	2.260	3.138	
TS01	2.035	2.619	2.243	2.295	2.412		2.041	2.575	2.243	2.275	2.358	
P01	2.035	3.582	2.253	2.286	2.087		2.045	3.580	2.237	2.268	2.096	
TS02	2.014	2.047	2.284	2.693	2.344		2.044	2.045	2.258	2.664	2.309	
P02	2.016	2.046	2.282	3.885	2.027		2.024	2.046	2.264	3.791	2.022	
R03	2.023	2.034	2.312	2.284	3.802		2.020	2.033	2.301	2.272	3.776	
TS03	1.983	2.533	2.301	2.301	2.295		2.003	2.503	2.286	2.285	2.251	
P03	1.996	3.770	2.306	2.288	2.047		1.998	3.827	2.294	2.276	2.044	
TS04	2.022	2.029	2.260	2.796	2.344		2.012	2.026	2.257	2.806	2.260	
P04	2.020	2.050	2.259	3.921	2.063		2.014	2.044	2.244	3.903	2.066	
R05	2.033		2.247	2.290	2.100	3.600	2.042		2.231	2.274	2.110	3.576
TS05	2.559		2.246	2.240	2.107	2.424	2.518		2.239	2.228	2.114	2.382
P05	3.537		2.246	2.253	2.076	2.102	3.521		2.234	2.237	2.083	2.110
TS06	2.000		2.252	2.677	2.100	2.399	2.021		2.228	2.643	2.100	2.357
P06	2.001		2.254	3.725	2.069	2.039	2.004		2.238	3.646	2.072	2.034
TS07	2.032		2.286	2.654	2.099	2.277	2.026		2.256	2.636	2.142	2.241
P07	2.037		2.283	3.850	1.986	2.068	2.036		2.263	3.729	1.990	2.078
R08	1.992		2.284	2.312	2.057	3.702	1.995		2.269	2.302	2.056	3.728
TS08	2.473		2.299	2.229	2.061	2.258	2.464		2.277	2.277	2.097	2.199
P08	3.676		2.304	2.286	2.003	2.043	3.746		2.289	2.270	2.007	2.049
TS09	1.986		2.246	2.892	2.074	2.366	1.979		2.243	2.892	2.067	2.288
R10	2.042	2.056	2.282		3.609	2.011	2.063	2.090	2.279		3.580	1.927
TS10	2.055	2.587	2.257		2.362	1.992	2.078	2.587	2.276		2.270	1.965
P10[a]	2.049	3.482	2.257		2.079	2.009	2.080	3.481	2.258		2.106	1.917
TS11	2.031	2.661	2.301		2.480	1.985	2.060	2.642	2.303		2.481	1.896
P11	2.026	3.613	2.292		2.101	1.992	2.056	3.633	2.292		2.138	1.896
TS12	2.011	2.068	2.688		2.339	1.984	2.065	2.093	2.676		2.280	1.922
P12	2.005	2.064	3.996		2.040	1.983	1.996	2.020	3.957		2.061	2.045
R13	2.021	2.027	2.298		3.632	2.023	2.010	2.035	2.259		3.614	2.111
TS13	1.972	2.508	2.324		2.423	2.005	2.012	2.493	2.320		2.385	1.930
P13[a]	1.984	3.488	2.302		2.062	2.022	2.004	3.493	2.287		2.035	2.005
TS14	2.021	2.023	2.814		2.415	1.976	2.012	2.025	2.716		2.349	2.064
P14	2.021	2.034	3.939		2.080	1.959	2.030	2.028	3.927		2.032	1.992

[a]water and chloride are in the cis-conformation in the product complex of the reaction p10 while they are in the trans position in product p13.

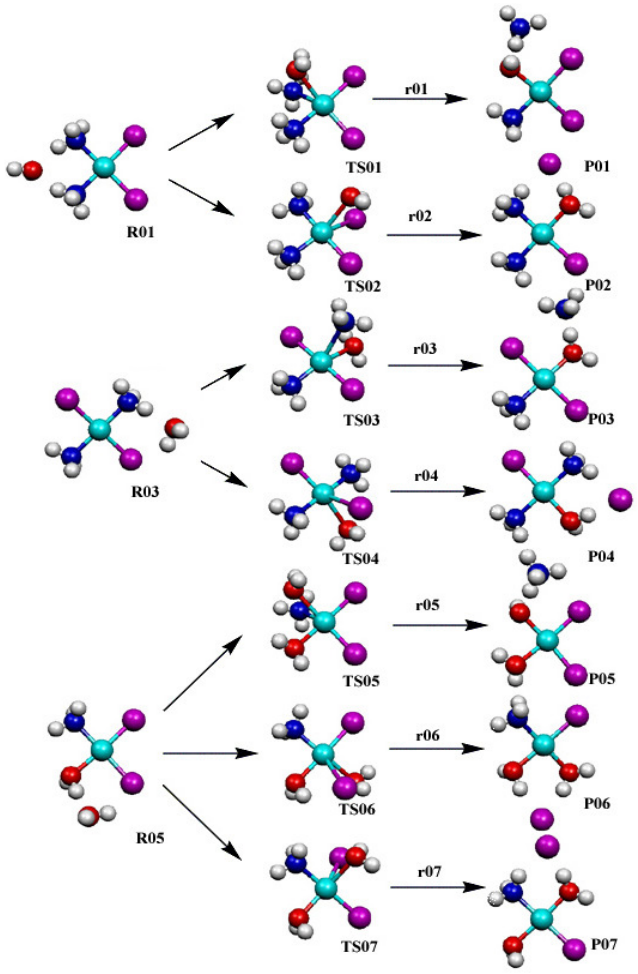

Figure 8. Optimized structures of reactants, transition states, and products in a supermolecular description of hydration reactions with the used reactions and supermolecules labeling.

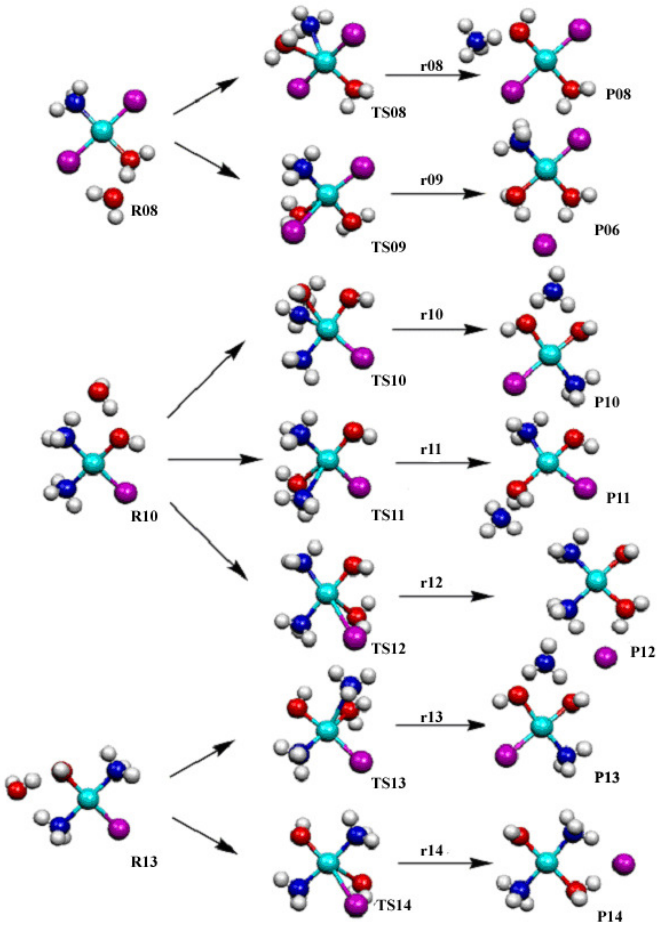

Figure 8. (cont.)

Table 4 collects the Pt-X distances of the transition structures. All of them have a shape of deformed trigonal-bipyramide. The bond distances between Pt and the entering and leaving ligands are substantially longer than the corresponding bond lengths in the reactant or product complexes. As discussed below, all of the hydration reactions are endothermic and in accord with the Hammond postulate, the TS structures resemble the products of the

reactions. This can be demonstrated for example by the fact that the bond distance for the arriving ligand (Pt-O) is always shorter than Pt-N for the departing ammine ligand despite the shorter Pt-N bonds in the stable complexes.

The Pt(II) structural data can be compared with the analogous data for the Pd(II) complexes which are summarized in the second part of Table 4. The most stable conformers of the reactants and products for Pd-containing supermolecules possesses a remote water, ammonia, or chloride oriented in the same manner as in the corresponding platinum complexes. Also, the relationship of the Pd-X bond lengths between metal and individual ligands are very close to the Pt analogues. Basically all of the structural similarities already discussed in the previous section as well as in other computational[102,120,121] and experimental[9,91,122,123] studies are also reflected in the Pd compounds.

7.2 Gibbs Energies of the Ligand Replacement and Association Energies

The reaction energies and Gibbs energies for the processes displayed in Figure 8 are collected in Table 5. In the upper part, the values for the platinum complexes are displayed. From the reaction energies and the Gibbs enthalpies, it can be seen that all of the hydration reactions are slightly endothermic. The hydration reaction requires energy of 8 – 21 kcal/mol. The estimated values for the Gibbs enthalpies approximately follow the reaction energies. In the case of chloride replacement, usually larger Gibbs enthalpies reflect the loss of energy from three rotational degrees of freedom of the chloride anion in comparison with a water molecule in reactants. To the contrary, the higher contents of vibronic energy of ammonium stabilize the products in the case of NH_3 detachment reactions. The role of a higher level of correlation contributions is obvious from a comparison of the MP2 and CCSD(T) columns of Table 5. While the dechlorination process does not exhibit any substantial deviations (maximum difference is 0.2 kcal/mol), the average decrease of the NH_3 detachment energy is about 1.6 kcal/mol. Nevertheless, even these changes are relatively very small. The differences in the MP2 and CCSD activation energies in the ΔE_a(Pt) and ΔE_a(Pd) columns in Table 5 have two sources: a) the corrections on the proper configuration of the reactant states (discussed below) and b) the differences

in the correlation energies at the both levels. The correlation energies at the CCSD(T) level are systematically lower by about 1.5 – 5.3 kcal/mol.

In all cases where the cis- and trans- diammine- or dichloro- conformers appear, the cis-structures are less stable due to the higher repulsion of both ligands in the cis-arrangement; thus, lower endothermicity of the reaction involving the cis-conformers can be noticed. For example, comparing the cisDDP+H_2O and transDDP+H_2O complexes (reactants in the first hydration step), the trans-conformer is about 12 kcal/mol more stable. The relative stability of the supermolecules can be obtained from the generalized hydration hypersurface defined above. The reference zero energy was set in this case for the most stable system: trans-$Pt(NH_3)_2Cl(OH)$+H_2O. This second step reactant is derived from the trans-$[Pt(NH_3)_2Cl(H_2O)]^+$ product complex replacing water with an OH^- group in order to keep the supermolecules neutral in this reaction branch. The higher stabilization of this reactant complex is due to the stronger electrostatic interaction of the Pt atom with OH^- ligand. Such a replacement can be considered to be a reaction caused by the increased pH of the environment.[124]

The generalized hydration surface is drawn in Figure 9. The ordering of the cis/trans conformers is apparent, as discussed above. From Figure 9, it can be seen that the most stable (final) product of hydration is the mixed cis-$Pt(NH_3)Cl(H_2O)(OH)$+NH_3 (r13) complex. The trans-$Pt(NH_3)Cl(H_2O)(OH)$ +NH_3 supermolecule lies about 4 kcal/mol higher followed by the trans-$Pt(NH_3)_2(H_2O)(OH)$+Cl (about 5 kcal/mol) and the cis-$Pt(NH_3)_2(H_2O)(OH)$+Cl (8 kcal/mol) complexes. Hence, the mixed monoammine-monochloro-diaqua-platinated complexes and the diammine-diaqua-complexes are lying in near proximity on the potential energy surface as can be seen in the above sections for both of the isolated Pt(II) and Pd(II) complexes. It was established that the most stable complex on the hydration surface of both metals is cis-$[Px(NH_3)Cl(OH)_2]^-$. In the present study, the most stable hydration product is cis-$Px(NH_3)Cl(H_2O)(OH)$. It is evident that the character of the mixed monoammine-monochloro-complex is preserved. The difference is caused by the fact that only neutral supermolecules were investigated in this section. Thus, no extra electrostatic work, which is necessary for the separation of the two (charged) particles to infinity, appears in the current scheme. This is also the reason why all of the reaction energies can be found in a relatively narrow range (within 12 kcal/mol), while differences up to 200 kcal/mol were observed in the previous

(thermodynamical) schemes which include also both cationic (2+, 1+) and anionic (2-, 1-) complexes.

Table 5. Reaction energies for the hydration of platinum complexes; subscript **r** denotes a reaction, and **a** denotes activation energies or Gibbs enthalpies. Index **c** means activation energies corrected on the proper reactant conformer.

	Gas-phase						**COSMO**	
	MP2				CCSD(T)		CCSD(T)	
	ΔE_r(Pt)	ΔG_r(Pt)	ΔE_a(Pt)	ΔG_a(Pt)	ΔG_r(Pt)	ΔE_a(Pt)	ΔG_r(Pt)	ΔE_a(Pt)
r01	10.1	9.5	32.8	30.2	8.7	28.9	12.8	32.3
r02	10.5	11.4	29.0	29.7	10.2	26.3[c]	6.7	22.7[c]
r03	15.0	14.6	36.2	33.1	13.8	33.6	11.5	31.1
r04	17.9	19.3	31.2	32.2	17.8	29.4	9.4	21.5
r05	17.0	15.7	39.2	35.9	15.2	30.2 [c]	10.1	30.9[c]
r06	9.5	10.0	30.5	30.6	9.7	28.4	7.0	24.7
r07	19.2	19.0	37.6	37.7	18.6	29.4 [c]	12.6	25.4[c]
r08	21.8	20.5	45.1	41.9	19.9	37.4 [c]	12.9	32.6[c]
r06	16.8	17.6	36.2	36.8	16.9	34.0	11.4	26.5
r10	12.8	12.4	34.3	32.7	11.5	30.6	10.9	35.8
r11	13.8	13.0	39.7	35.9	12.4	30.4 [c]	9.4	33.6[c]
r12	16.2	16.5	31.4	31.8	16.5	26.0 [c]	8.4	24.5[c]
r13	17.3	17.2	42.2	40.1	15.2	38.2	12.2	35.1
r14	20.7	20.7	36.2	35.7	20.6	29.3 [c]	10.7	24.6[c]
	ΔE_r(Pd)	ΔG_r(Pd)	ΔE_a(Pd)	ΔG_a(Pd)	ΔG_r(Pd)	ΔE_a(Pd)		
r01	6.1	6.3	21.5	20.1	5.2	18.3		
r02	9.5	11.0	20.3	21.3	9.8	18.2 [c]		
r03	12.1	11.9	26.6	24.6	11.0	23.7		
r04	18.0	19.3	23.4	24.5	17.7	21.8		
r05	18.9	18.7	27.4	27.4				
r06	9.4	10.0	22.6	22.9				
r07	13.5	12.1	28.2	25.1				
r08	18.0	16.9	31.9	29.4				
r06	16.6	17.4	29.3	29.8				
r10	9.5	9.0	22.1	20.7				
r11	9.9	9.0	27.6	24.8				
r12	13.6	16.3	22.1	22.3				
r13	16.4	13.9	33.4	27.7				
r14	17.9	16.3	30.0	27.1				

[x] rXY labels are taken from Figure 8.

This conclusion matches well with the experimental data.[125] In the work of Jestin et al.,[39] the cis-diammine-chloro-aqua-complex was considered for direct coordination with the N_7-site of the DNA base. The replacement of the aqua-ligand with guanine was found to be substantially faster than the formation of the diaqua-Pt(II) complex.

The obtained hydration energies can be compared with the values of experimentally determined equilibrium constants published in studies for both cisplatin[26] and transplatin.[27] These constants were determined at 318.2 K in a 0.1 M $NaClO_4$ solution in pH 2.8−3.4, as mentioned in the Introduction section, and correspond to ΔG = 1.5 and 2.1 kcal/mol for cisplatin and transplatin, respectively. Clearly, the present values are larger (cf. Table 5). Nevertheless, relative agreement should be noticed. The equilibrium constants for the second hydration step of cis-/trans-$[Pt(NH_3)_2(H_2O)_2]^{2+}$ cannot be compared directly since we did not consider the charged complexes. The published experimental equilibria[26,27] correspond to ΔG = 2.3 and 3.0 kcal/mol. Despite the differing total charge, the qualitative accordance with hydration of the $[Pt(NH_3)_2(H_2O)(OH)]^+$ complexes is preserved. Nevertheless, the mixed $Pt(NH_3)Cl(H_2O)(OH)$ structures were found to be thermodynamically more stable. This is caused by the omitted environmental effects in the model used. The results for the improved models are presented in the next section.

The reaction energies and the Gibbs enthalpies for hydration of the Pd(II) complexes are summarized in the lower part of Table 5. In this case, only the first hydration step was evaluated at the CCSD(T) level due to the large amount of computational time necessary for such simulations and only minor differences in the reaction energies in comparison with the MP2 results. All of the reaction energies of the palladium complexes show endothermic character similar to the cis-/transplatin complexes, and even the absolute values strongly resemble the solvation of these complexes. The largest difference is about 3.9 kcal/mol and an average difference of approximately 1.8 kcal/mol (at the MP2 level). The numbers are really convincing concerning the extended similarity of the reaction surface or landscape (in ΔG). This is also in agreement with the previous parts and related studies.[102,120,121] Practically, the whole previous energy discussion in this section concerning the Pt(II) hydration applies also to the Pd(II) reactions. If the generalized hydration surface is drawn in the same manner into Figure 9, "Pd/Pt degeneracy" of the reactants and products energies

would be clearly seen, with the exception of the energies of the TS structures.

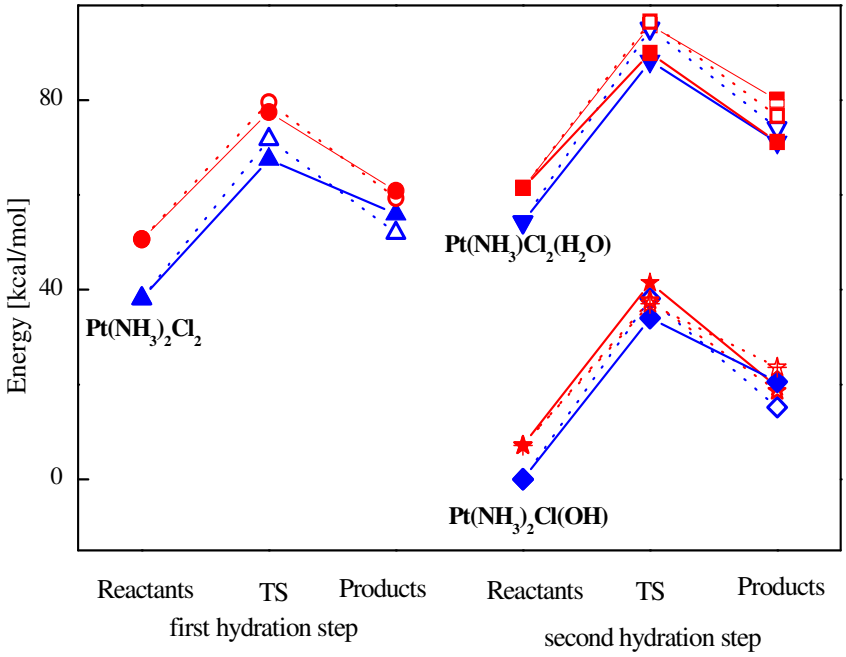

Figure 9. The generalized hydration energy surface for Pt(II) complexes at the CCSD(T) level. Two different parts in the 2nd hydration step are connected with two different types of reactants (with water and with the hydroxyl group): ♦ and ▲ belong to trans-reactants; ●,■, and * to cis-reactants; solid and half-filled symbols connected with solid lines label dechlorination; open or open with cross symbols and dotted lines designate ammonia detachment.

The strength of the association interactions of the two parts of a supermolecule has been examined and is summarized in the first (gas-phase) column of Table 6 where three sections related to different remote ligands (water, ammonia, and chloride) are present. Surprisingly, the water associates are not usually as strongly bonded as the ammonia complexes in the product states. An explanation of the lower water association energies can be derived from the fact that polarized water, as a coordinated ligand,

makes stronger H-bonds with remote molecules than Pt-polarized NH_3 ligands. Such a conclusion is also confirmed by the fact that, for instance, leaving ammonia in a product state of trans-$Pt(NH_3)Cl_2(H_2O)$ forms H-bonds more preferably (by 5 kcal/mol) with H_2O and Cl ligands than with NH_3 and Cl. In the reactant part of Table 6, higher association energies can be observed in the case of the second hydration step where one ligand of the solvent (H_2O or OH^-) is already coordinated to Pt. There is no substantial difference in the association energies when a remote water interacts with a neutral water-ligand or hydroxyl anion as follows from the data of the R05 and R08 rows or of the R10 and R13 rows of Table 6. Similarly, the association energies of NH_3 are not influenced in such cases, too. The relatively large association energies for the remote chloride species are a consequence of the separation of charged particles (Cl^- and 1+ charged Pt-complex), that is, the result of electrostatic work. This situation resembles closely the determination of the hydration energies in the sections with isolated Pt(II) and Pd(II) complexes above where the charged molecules and particles were considered. The electrostatic work would be substantially diminished in any polarized solvent, especially in a water environment where efficient screening is present.[126]

7.3 Activation Energies and Estimation of Rate Constants

All of the Pt transition states adopt five-coordinated trigonal-bipyramidal structures, which lie more than 25 kcal/mol above the energy of the reactant supermolecules on the potential energy surface. In Table 5, the last two columns in the MP2 part and the last column of the gas-phase CCSD(T) sections collect the activation energies of TS for the studied hydrations.

The lowest activation barrier was predicted for the cisplatin hydration when the first and then second chloride anions are replaced (about 26 kcal/mol). Thus, these dechlorinations represent the fastest reactions considered here. Moreover, the first step is one of the less endothermic processes (ca. 9 kcal/mol) in the whole hydration scheme. The highest barriers (more than 35 kcal/mol) were calculated for the formation of the trans-$PtCl_2(H_2O)_2$+NH_3 and trans-$Pt(NH_3)Cl(H_2O)(OH)$+NH_3 complexes. Based on the MP2 activation energies of the Pt complexes, the replacement of the ammonium ligand should always be slower than the dechlorination process. Thus, a kinetic factor would prevail, and the chloride anions would be preferentially replaced. However, this hypothesis was not completely and unambiguously confirmed by the CCSD(T) calculations. The activation

energies even at the CCSD(T) level are still always higher for the ammonium detachment, but the differences sometimes markedly diminish.

Table 6. The association energies between both parts of the supermolecule (in kcal/mol); an asterisk (*) labels the two reactions where the deammination product supermolecule contains a neutral NH_3 molecule and an NH_4^+ cation in the COSMO calculations; NH_3 was obtained in all corresponding gas-phase products; all energies are BSSE-corrected with inclusion of deformation contributions.

H_2O+ reactant	Gas-phase	COSMO
R01	-10.4	-5.8
R03	-9.2	-2.9
R05	-13.8	-7.4
R08	-12.7	-7.4
R10	-12.7	-8.3
R13	-13.5	-8.8
NH_4 + product		
P01	-15.6	-12.7
P03	-14.7	-16.3*
P05	-15.0	-11.0
P08	-16.5	-16.7
P10	-15.8	-15.7
P11	-11.6	-13.6*
Cl^- + product		
P02	-112.5	-8.3
P04	-116.9	-5.4
P06	-121.0	-9.0
P07	-117.0	-4.8
P12	-109.5	-2.4
P14	-111.5	-1.9

An estimation of the TST rate constants was performed from the determined structures, energies, and vibrational modes of all of the reaction components. These constants are collected for both directions of the reactions (k_1, k_{-1}, k_2, and k_{-2}) at temperature 310 K in Table 7. Comparing the calculated constants for the dechlorination process in the 1st hydration step with the available experimental values,[25,39,124] a qualitative agreement has been reached. It is clear that differences of several orders of magnitude in the values of the rate constants represent a variation of only a few kcal/mol on the hydration surface. Hence, the requirement for accuracy for such kinetic quantity is at the limit of the current computational techniques for the

examined systems. From a comparison of forward and backward rate constants, it follows that neither the height of the activation barrier nor the geometry of TS (its location on the energy surface) are sufficiently accurate for quantitative assessments.

In the lower section of Table 5, the energy characteristics of the palladium transition states are collected. One can notice that the Pd activation barriers are substantially lower than the corresponding barriers for hydration of the Pt(II) complexes. The average difference between the corresponding barriers is about 10 kcal/mol. The smallest difference of 6.2 kcal/mol occurs in the second chloride replacement of the trans-$Pt(NH_3)_2Cl(OH)$ structure.

It should be mentioned that the global minima on the reactant side do not always coincide with the conformation from which the hydration process starts. For example, for chloride replacement of cisplatin, the global minimum structure must be transferred to the conformation where water is H-bonded simultaneously to ammonium and chloride (about 0.5 kcal/mol higher). In this case, it is expected that the relatively fast movement of the (remote) water molecule over the metal complex can occur, and the required conformation is temporarily available. Such "water transfer" does not represent a reaction bottleneck and will not slowdown the whole hydration process. This assumption is based on the fact that the corresponding minimum (the proper conformation of the given reactant) is energetically close to the global minimum (less than 5 kcal/mol in all considered cases). Since the water transfer is connected only with H-bond reformation, which is weak in comparison with the dative bond rearrangements, the energy of TS between such H-bonded minima is not high. Moreover, in reality, usually more water molecules can be expected in the vicinity of the platinum complex. Nevertheless, these considerations are very important for a correct estimation of the rate constants which are very sensitive (exponentially) to any energy change. Consequently, if the activation energies are only slightly lower (up to 4 kcal/mol), the rate constants are reduced by nearly two orders of magnitude. A complete set of rate constants for hydration of cis-/transplatin together with the results for the first solvation step of the analogous Pd complexes and some experimentally known values are summarized in Table 7. The average difference corresponds to 10^6 times shorter reaction time for the hydration of palladium complexes (Table 7). This conclusion is in good accord with the experimental findings for the

reactions with DNA bases where palladium complexes are expected to interact roughly 10^4 times faster than platinum(II) complexes.[9]

Table 7. Forward (k_1, k_2) and backward (k_{-1}, k_{-2}) rate constants estimated from TST at T = 310 K.

	Gas-phase				**COSMO**	
	Pt(MP2)		Pt(CCSD)		Pt(CCSD)	
	k_1	k_{-1}	k_1	k_{-1}	k_1	k_{-1}
r 01[a]	3.6e-09	1.9e-02	2.0e-06	1.1	1.7e-09	1.9
r 02	7.0e-09	8.3e-01	5.1e-07	17.7	1.3e-04	84.
exp.[a]					1.9e-04	6.0e-02
exp.[c]					5.2e-05	7.6e-03
exp.[d]					1.1e-04	
r 03	3.2e-11	6.1e-01	2.0e-09	5.9	1.1e-08	1.7e-01
r 04	1.1e-10	4.7e+03	2.1e-09	7.5e+04	5.4e-04	3.1e+02
exp.[b]					1.1e-03	2.2
	k_2	k_{-2}	k_2	k_{-2}	k_2	k_{-2}
r 05	3.5e-13	4.1e-02	7.1e-07	1.4	2.7e-10	5.5e-01
r 06	1.7e-09	2.0e-02	4.9e-08	7.7e-01	2.1e-04	8.8e-01
r 07	1.7e-14	4.1e-01	1.0e-08	3.4e+01	5.6e-07	5.4e+01
r 08	1.9e-17	5.5e-03	5.7e-12	2.4e-01	9.5e-09	2.2e+00
r 09	9.2e-14	1.1	3.4e-12	4.9e+01	3.5e-04	7.7e+02
r 10	5.5e-11	3.1e-02	2.1e-08	5.3e-03	4.5e-10	6.3e-03
r 11	3.4e-13	5.0e-04	1.2e-06	2.6e-01	2.6e-09	1.7e-01
r 12	2.4e-10	1.1e+02	1.6e-06	2.2e+03	***4.4e-06***	1.4e+01
exp.[a]					***2.3e-04***	9.9e-01
exp.[e]					8.0e-5	
exp.[f]					2.0e-5	
r 13	3.9e-16	5.0e-04	2.7e-13	2.9	3.8e-11	3.1e-01
r 14	4.5e-13	1.7e+02	3.2e-08	4.7e+03	***2.4e-04***	1.0e+02
exp.[b]					***4.0e-06***	2.0e-04
	Pd(MP2)		Pd(CCSD)			
	k_1	k_{-1}	k_1	k_{-1}		
r 01[a]	4.6e-02	1.3e+03	8.2	5.2e+04		
r 02	5.3e-03	3.6e+05	1.6e-01	1.6e+07		
r 03	2.9e-05	6.7e+03	3.1e-03	1.2e+05		
r 04	3.1e-05	1.4e+09	4.4e-04	1.0e+10		

[a]ref.[26]; [b]ref.[27]; [c]ref.[25]; [d]ref.[39]; [e]ref.[134]; and [f]ref.[135].

8. Changes in the Thermodynamic and Kinetic Parameters under the Effects of Solvation

In the last section, the influence of the adjacent molecules is examined. The applied computational model is based on the same supermolecular approach as above considering the molecular complexes to be neutral and in the singlet electronic ground state.

Since the dominant effect of the solute-solvent interaction (at least in the case of water solution) is of electrostatic origin, one possible approach used to study such phenomena is to replace the explicit solvent molecules by a dielectric continuum. This continuum is represented by polarization charges appearing on finite-sized elements on the boundary surface between the solute and the continuum.[127] This is the common description for the whole class of the so-called "Apparent Surface Charge" methods (ASC). The COSMO method belongs to this ASC group. The improvement of COSMO is its better description of systems in solvent with high permitivity[128] so that it is suitable for the simulation of a water environment. The "United Atomic Topological Model" (UATM) was used for building the cavity. In UATM, hydrogen atoms are not surrounded by their own cavity sphere but are considered to be a subpart of the cavity sphere of the hydrogen-bonded atom. This strategy reduces the number of spheres and still provides high enough accuracy, as pointed by Tomasi[127,129] and Amovilli.[130] The second advantage of this choice is that the method is faster and has better convergence. The utilization of the supermolecular model for the hydration reaction of cisplatin within the UATM molecular cavity is schematically depicted in Figure 7.

The designed molecular complexes of the reactants, products, and transition states were optimized using the Becke3LYP functional of the DFT technique and the COSMO method. The used basis set is the same as in the previous *in vacuo* model. The single point energy determination was performed with the CCSD(T) method and the 6-31++G(d,p) basis set within the COSMO formalism. The active space contained all of the orbitals except those belonging to frozen core electrons (1s of the O and N atoms; inner electrons of Pt and Cl were covered within the ECP approach).

8.1 Structures of Supermolecules in the COSMO Model

The Pt-L distances in structures within the PCM approximation are summarized in Table 8. From the table, two basic features can be noticed.

First, all distances are increased under the solvent effects, which truly reflects the fact that some portion of electron density of the Pt-complexes is involved in the interactions with the surrounding solvent molecules in more realistic models. Comparing the gas-phase and COSMO models, the average difference in the Pt-L dative bonds is about 0.04 Å. Secondly, the largest differences in comparison with the gas-phase structures occur for the Pt-L distances between metal and the weakly bonded remote particles. This can be explained by the fact that these remote ligands are also attracted by the electrostatic charge induced on the cavity surface (simulating the interactions with solution). The largest difference in the molecular parameters occurs in the cisplatin+water complex. The main change can be seen in the shift of the H-bonded water from its position above the Pt-complex plane in the gas-phase case towards the plane in the COSMO case (cf. Figure 10a). Usually, weakly bonded particles (water, ammonium, or chloride) were stabilized in the complex plane in both the isolated and the COSMO structures. Arrangement with remote particles above the complex plane is very rare since sufficient additional stabilization is required in this case. Such a stabilization can be found in the R01 reactant in the gas-phase as mentioned above. There, the weak bonding interaction between one of the water protons and the platinum cation stabilizes the water molecule above the complex plane. Passing from the gas phase to the condensed phase model, this interaction was replaced by interaction of the water molecule with induced charges on the cavity surface.[126] The additional electrostatic forces diminish this Pt…H interaction so that the water molecule could not be kept above the Pt-plane and is transferred towards the complex plane.

It can be concluded that in analogy with the gas-phase results, the TS structures more closely resemble the products than the reactants which is in good accord with the Hammond postulate. The other related difference between the results of the gas phase and the COSMO approach reflects a partial change of the reaction coordinate in most of the cases of the deammination reactions (cf. Figure 10b). The ion-pair structures in the frame of the supermolecule are formed as the products in both hydration steps. The NH_4^+ ion is released from the platinum complex instead of the ammonia molecule. The extra proton is taken from the ligated water. The preference for the NH_4^+ cation is about 2.6 kcal/mol. Consequently, the difference between the gas-phase product conformers P10 and P13 disappears. The formation of the ion-pair structure is in good accordance with the quantum chemical calculations of the amino acids. There, the formation of the NH_2-

COOH structure represents the most stable arrangement in the gas-phase calculations, while the NH_3^+ - COO^- zwitterions become the global minima in studies employing PCM techniques. This was for the first time mentioned by Tomasi[131] for glycine and later also confirmed by others.[132,133] Except the different character of the product, the transfer from NH_3 to NH_4^+ does not substantially change the position of the remote ligand. As is demonstrated in Table 8 and Figure 10b, the remote ligand remains in a very similar location in both the gas-phase and the COSMO models.

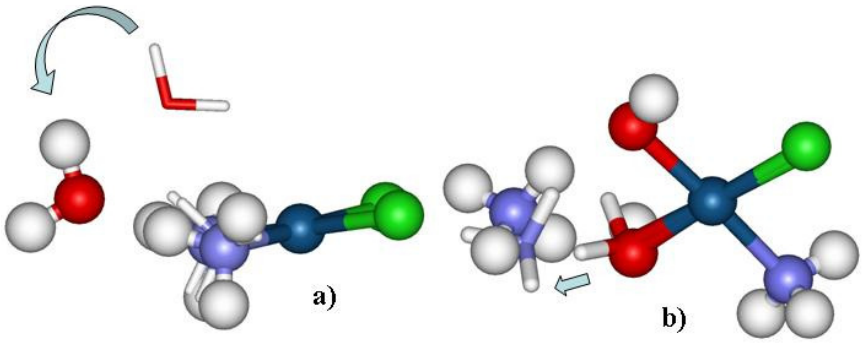

Figure 10. Superimposed optimized geometries from the gas-phase and COSMO calculations for: (a) the reactant supermolecule of the hydration process r01: cis-$Pt(NH_3)_2Cl_2$+H_2O; arrow points to the change of water position passing from the gas-phase (thin sticks) to the PCM structure (balls&sticks), (b) the product supermolecule p10: neutral (gas phase – thin sticks) and ion pair structures (PCM – ball&sticks). Arrow shows the proton transfer from an aqua-ligand to a released NH_4^+ particle.

8.2 Thermodynamics and Activation Energies

The complete reaction Gibbs free energies of the hydration processes and their activation barriers calculated at the CCSD(T) level are summarized in the COSMO section of Table 5. At first glance, one can notice that practically all of the hydration energies are reduced by several kcal/mol in comparison with the gas-phase results. The reaction energies are usually slightly less endothermic for the chloride replacement. The lowest ΔG hydration energies are predicted in both steps of cisplatin dechlorination: 6.7 and 8.4 kcal/mol. On the contrary, the deammination of cisplatin is

accompanied by the largest endothermicity increase of approximately 12.8 kcal/mol in the first step and 12.9 kcal/mol in the second step. Such trends were not observed in the gas-phase calculations. Moreover, the lowest Gibbs energy in the gas-phase is connected with the deammination processes r01 (8.7 kcal/mol) and r10 (8.1 kcal/mol).

The predicted energies of the first hydration-dechlorination step (r02 and r04) can be compared with the value of $\Delta G = 3.1$ kcal/mol for cisplatin and $\Delta G = 4.1$ for transplatin obtained from experimental studies[26,27] and evaluated from the equilibrium constants determined as $pK_1 = 2.19$ and 2.92 for both cis- and transplatin, respectively. It can be seen that the inclusion of environmental effects substantially improves the predicted energies. The deviation of about 3 – 5 kcal/mol can be considered as an error bar of the model used for the calculations, and some uncertainty should be connected with the determination of the experimental values of pK. A similar comparison can be done for the second step, hydration processes r12 and r14, combining reactions K_{a3}-K_2-K_{a1} from eqs. 1 and 2. The evaluation of the corresponding Gibbs energies gives $\Delta G_2^* = \Delta G_2 + \Delta G_{a1} - \Delta G_{a3}$ (assuming the same temperature T = 310 K in all three measurements). In this way, the Gibbs energies $\Delta G_2^* = 3.4$ and 4.6 kcal/mol can be predicted for cis- and transplatin, respectively. Here however, the uncertainty in the "experimental" ΔG_2^* values is substantially higher. One can conclude that, despite the fact that the calculated energies do not match exactly the experimental data, the appropriate trend in going from the gas-phase to the COSMO values is obtained.

Comparing the above results with the analogous data of Zhang,[110] very good agreement can be observed. However, since the latter study assumed a slightly different charged reactant (cis-$[Pt(NH_3)_2Cl(H_2O)]^+$+H_2O) for the second hydration step, a somewhat higher reaction energy of 14.1 kcal/mol is obtained compared to our value of 7.8 kcal/mol (or $\Delta G = 8.4$ kcal/mol) for the neutral complex of cis-$Pt(NH_3)_2Cl(OH)$+H_2O. This is in very good accord with the lower stabilization of cisplatin in the diaqua than the aqua-hydroxo-form as demonstrated already in previous sections.

The last column of Table 5 contains information about the reaction barrier heights. The differences between the energies of the optimized TS structures and their reactant conformers, which were obtained going downhill from these TS (using the Intrinsic Reaction Coordinate (IRC) algorithm), were used for the determination of the activation energies at the CCSD(T) level of calculation. It is obvious (the last column of Table 5) that

Table 8. The optimized Pt-L distances between Pt and the N, O, or Cl atom (in Å) in the COSMO model and a comparison with gas-phase results from Table 4. Structures P06 = P09, P10 = P13.

	COSMO						differences between PCM and gas-phase					
	Pt-N	Pt-N	Pt-Cl	Pt-Cl	Pt-O	Pt-O	Pt-N	Pt-N	Pt-Cl	Pt-Cl	Pt-O	Pt-O
R01	2.065	2.065	2.361	2.361	3.862	-	0.015	0.015	0.084	0.084	0.679	
TS01	2.052	2.617	2.362	2.339	2.365	-	0.017	-0.003	0.119	0.044	-0.047	
P01	2.052	3.735	2.369	2.367	2.040	-	0.017	0.153	0.116	0.081	-0.047	
TS02	2.058	2.045	2.354	2.798	2.467	-	0.044	-0.002	0.070	0.105	0.123	
P02	2.070	2.034	2.350	4.083	2.082	-	0.054	-0.012	0.067	0.198	0.055	
R03	2.063	2.064	2.369	2.348	3.961	-	0.040	0.030	0.057	0.064	0.159	
TS03	2.030	2.592	2.357	2.361	2.366	-	0.047	0.059	0.056	0.060	0.071	
P03	2.036	3.898	2.357	2.352	2.069	-	0.040	0.128	0.051	0.064	0.022	
TS04	2.055	2.058	2.344	2.799	2.421	-	0.033	0.029	0.084	0.003	0.077	
P04	2.067	2.062	2.321	4.092	2.096	-	0.047	0.012	0.062	0.171	0.033	
R05	2.056	-	2.363	2.322	2.099	3.798	0.023		0.116	0.032	0.000	0.198
TS05	2.603	-	2.332	2.311	2.108	2.358	0.044		0.086	0.071	0.001	-0.066
P05	3.809	-	2.317	2.362	2.106	2.028	0.272		0.071	0.109	0.030	-0.074
TS06	2.035	-	2.340	2.890	2.106	2.385	0.035		0.088	0.213	0.006	-0.014
P06	2.025	-	2.312	3.938	2.098	2.089	0.024		0.058	0.213	0.029	0.050
TS07	2.049	-	2.352	2.741	2.118	2.369	0.017		0.066	0.087	0.019	0.093
P07	2.065	-	2.345	4.031	2.036	2.065	0.027		0.062	0.180	0.050	-0.003
R08	2.028	-	2.357	2.338	2.094	3.757	0.036		0.073	0.026	0.037	0.055
TS08	2.364	-	2.350	2.352	2.130	2.487	-0.110		0.051	0.123	0.069	0.230
P08	3.855	-	2.357	2.357	2.116	1.9863	0.179		0.053	0.071	0.113	-0.057
TS09	2.015	-	2.336	2.822	2.096	2.417	0.029		0.090	-0.070	0.022	0.051
R10	2.068	2.074	2.360	-	3.738	2.021	0.026	0.018	0.078		0.129	0.010
TS10	2.077	2.658	2.342	-	2.351	2.008	0.022	0.071	0.085		-0.011	0.016
P10	2.058	3.519	2.369	-	2.038	2.044	0.009	0.037	0.112		-0.041	0.035
TS11	2.056	2.673	2.363	-	2.463	2.000	0.025	0.012	0.062		-0.017	0.015
P11	2.057	3.926	2.358	-	2.100	1.988	0.031	0.313	0.066		-0.001	-0.004
TS12	2.057	2.094	3.009	-	2.405	2.003	0.046	0.026	0.321		0.066	0.020
P12	2.087	2.026	4.104	-	2.086	2.005	0.082	-0.038	0.107		0.046	0.022
R13	2.066	2.060	2.371	-	3.740	2.032	0.045	0.033	0.073		0.108	0.009
TS13	2.025	2.717	2.390	-	2.249	2.017	0.053	0.209	0.066		-0.174	0.012
TS14	2.056	2.057	2.873	-	2.553	1.998	0.034	0.035	0.059		0.138	0.023
P14	2.061	2.060	4.093	-	2.119	1.986	0.039	0.026	0.154		0.039	0.027

all of the dechlorination reactions have substantially lower reaction barriers than the corresponding deammination processes. This trend is also partially notable from the gas-phase results; however, in solvent, it is much clearer

and unambiguous. The relatively large difference between dechlorination and deammination occurs in the first hydration step, about 10 kcal/mol for both cis-/transplatin complexes. In the second step, the difference is slightly smaller but still remains over 6 kcal/mol. These differences distinctly speak out for the kinetic preference of the dechlorination process (cf. discussion below).

For the deammination processes (with exclusion of the r04 and r11 reactions) the ligand exchange and the proton transfer from water to ammonia occur simultaneously within the reaction course. However, the heights of the activation barriers are not affected by this fact, since the proton transfer starts on the reaction coordinate a little later after passing the TS structure, going already downhill towards the products on the energy surface.

The association energies of platinum complexes with water, ammonia, or chloride species were determined at the CCSD(T)/6-31++G(d.p) level. The obtained results are collected in the second (COSMO) column of Table 6. The obtained values can be compared with the gas-phase calculations. It is apparent that the H-bond interactions of a water molecule with the Pt-complex are decreased in the COSMO model, on average by about 5 kcal/mol. In the case of the NH_3/NH_4^+ detachment, the changes are practically negligible (4 kcal/mol at most). The products of the dechlorination processes represent the most striking cases since the remarkable reduction of the association energies was achieved. The explanation can be deduced from the efficient screening of the electrostatic interaction between the positively charged platinum complex and the chloride ligand. However, this fact does not mean that the electrostatic forces were diminished since other Coulombic interactions based on the interaction between the monomers and the induced charges on the cavity boundaries were introduced. These induced charges realistically simulate the effect of the solvent environment. Therefore it can be assumed that the bulk water environment efficiently compensates the electrostatic work, which is necessary for the separation of the two charge carriers (the Cl^- anion and $[Pt\text{-}complex]^+$ as well as the NH_4^+ cation and $[Pt\text{-}complex]^-$).

8.3 Evaluation of the Rate Constants

The TST rate constants, determined according to eq. 5, are collected in the last two columns of Table 7. The rate constants for the hydration-dechlorination processes in the first step are generally about four orders of

magnitude higher than the corresponding values for the deammination reaction. For the replacement of the second water molecule, the difference decreases but still remains about three orders of magnitude higher. It means that dechlorination reactions are kinetically preferred over deammination reactions. The detection of the process, where ammonium is released, would be very difficult in real experimental conditions since very low concentration of cisplatin (usually about 5 μM) is used.

For a comparison with experimental measurements, there are several results available.[25-27,39] From Table 7, it follows that a very good agreement with the experimental data was achieved. The differences are within an order of magnitude for the forward reaction and slightly worse for reverse processes. For the second dechlorination step, reactions r12 and r14, agreement with the published measurements is also fairly good, but here slightly different reactions are considered. Unfortunately there are no data for the evaluation of kinetic parameters such as ΔG_2^* in the thermodynamic part. Nevertheless, the rate constants for the second step are not too far from the experimental data, and substantial improvement of the results obtained with the COSMO model in comparison with the *in vacuo* calculation was achieved.

A comparison with other theoretical studies devoted to similar systems[110-112] can be performed, at least for dechlorination reactions. Besides cisplatin, the ethylenediammine-dichloro-Pt(II) complexes were also studied. Zhang et al.[110] have estimated the energetic and kinetic parameters from a similar model, employing several PCM models and the DFT calculation with a double-zeta quality basis set and with the pseudopotential approach. Their results are in a very good accord with the relevant part of the present data. Similarly, de Costa et al.[111,112] made estimations of rate constants for $Pt(en)Cl_2$ dechlorination reactions combining the general Born-Onsager SCRF or PCM models with the DFT or MP2 level of theory. They reported activation barriers of 32 and 23 kcal/mol for gas-phase and PCM, respectively. Also, their rate constants are fairly close to our results (k_1 = 1.9e-11 for gas-phase and k_1 = 4.8e-5 for PCM). This similarity originate, to a large extent, from the chemical propinquity (or relations) of those Pt(II) complexes

9. Conclusions

Recent progress in computational methodologies and improvements in computational facilities allow new insight into many biological processes to be obtained by the accurate, ab initio calculations. Among such processes is the biological activity of cisplatin reviewed in this chapter. The essential results could be summarized as follows:

- There are no substantial differences in the thermodynamic behavior of cis and trans isomers during the hydration process.
- The most stable products of hydration reactions are $[PtCl(NH_3)(OH)_2]^-$ and $Pt(NH_3)_2(OH)_2$. These results are in partial agreement with the experimental findings that the hydrated products of cis-DDP contain two ammonia (and two solvent molecules) coordinated to the Pt atom.
- The significant similarity of the thermodynamic parameters of the square-planar Pt(II) and Pd(II) complexes was predicted. Since there is considerable difference in the biological activity it is concluded the Pd and Pt compounds do not fulfill the QSAR principle.
- Reaction barriers were determined from the TS structures. In agreement with many experimental findings, the activation energies are distinctly lower for palladium complexes than for the corresponding Pt structures; the average difference is 9.7 kcal/mol, which indicates that the hydration processes are about 10^6 times faster in the palladium case. This is 1-2 orders of magnitude more than the values obtained from experimental data.
- Combining the PCM approach with the gas phase methodology is the most promising way to understand and model the effect of a water solution. The COSMO model was used for the determination of the interaction energies and the activation barriers at the CCSD(T)/6-31++G(d,p) level.
- The endothermicity of the hydration reactions was confirmed. The Gibbs energies amount to $\Delta G = 6.7$ and 12.8 kcal/mol for the chloride and ammonium replacements of the water. Analogous values for transplatin are 9.4 and 11.5 kcal/mol. These dechlorination results match the experimental data fairly accurately.
- The activation of cisplatin can be regarded purely based on thermodynamic properties. Since the stabilization energies are lowered within each hydration step by about 10 kcal/mol the hydrated complexes become less stable, it means more reactive.

• The determined rate constants of the dechlorination process are by several (3-4) orders of magnitude larger than those for the deammination process. Very good agreement with the available experimental data was achieved.

• The thermodynamically most stable products from the first and second sections (the $[PtCl(NH_3)(OH)_2]^-$ $[PdCl(NH_3)(OH)_2]^-$ complexes) will be formed with very low probability due to the discriminating kinetic factors for the deammination process.

Acknowledgment

The study was supported by NSF-MŠMT grant No. 1P05ME784(JVB), grant GAUK No. 2003/181/B_CH(JVB), project MSM 0021620835 (JVB), NIH grant S06 GM008047(JL), NSF-CREST grant HRD-0318519(JL), ONR grant N00034-03-1-0116(JL), grant 203/05/0009, the Grant Agency of the Czech Republic (JS) and AVOZ5 0040507, MŠMT CR (JS). The authors thank the Meta-Centers in Prague (Charles University and Czech Technical University), Brno (Masaryk University) and Pilsen (University of West Bohemia) for the generous support of the computational resources.

References

(1) Rosenberg, B.; Van Camp, L.; Trosko, J. L.; Mansour, V. H. *Nature* **1969**, *222*, 385.
(2) Cohen, S. M.; Mikata, Y.; He, Q.; Lippard, S. J. *Biochemistry* **2000**, *39*, 11771.
(3) Lilley, D. M. J. *J. Biol. Inorg. Chem.* **1996**, *1*, 189.
(4) Coste, F.; Malinge, J. M.; Serre, L.; Shepard, W.; Roth, M.; Leng, M.; Zelwer, C. *Nucleic Acids Res.* **1999**, *27*, 1837.
(5) Ziegler, C. J.; Sandman, K. E.; Liang, C. H.; Lippard, S. J. *J. Biol. Inorg. Chem.* **1999**, *4*, 402.
(6) Djuran, M. I.; Lempers, E. L. M.; Reedijk, J. *Inorg. Chem.* **1991**, *30*, 2648.
(7) Lempers, E. L. M.; Reedijk, J. *Inorg. Chem.* **1990**, *29*, 217.
(8) Barnham, K. J.; Djuran, M. J.; Murdoch, P. d. S.; Ranford, J. D.; Sadler, P. J. *Inorg. Chem.* **1996**, *36*, 1065.
(9) Barnham, K. J.; Bauer, C. J.; Djuran, M. I.; Mazid, M. A.; Rau, T.; Sadler, P. J. *Inorg. Chem.* **1995**, *34*, 2826.

(10) Barnham, K. J.; Djuran, M. J.; Murdoch, P. d. S.; Sadler, P. J. *J. Chem.Soc., Chem. Commun.* **1994**, 721.
(11) Kleine, M.; Wolters, D.; Sheldrick, W. S. *J. Inorg. Biochem.* **2003**, *97*, 354.
(12) Teuben, J.-M.; Reedijk, J. *J. Biol. Inorg. Chem.* **2000**, *5*, 463.
(13) Peleg-Shulman, T.; Gibson, D. *J. Am. Chem. Soc.* **2001**, *123*, 3171.
(14) Treskes, M.; Holwerda, U.; Nijtmans, L. G.; Pinedo, H. M.; van der Vijgh, W. J. F. *Cancer Chemother. Pharmacol.* **1992**, *29*, 467.
(15) Reedijk, J.; Teuben, J. M. "Platinum-Sulphur Interaction Involved in Antitumor Drugs, Rescue Agents and Biomolecules." In *Cisplatin*; Lippert, B., (ed.); Wiley-VCH: Weinheim, 1999.
(16) Bierbach, U.; Farell, N. *J. Biol. Inorg. Chem.* **1998**, *3*, 570.
(17) Beltran, M.; Onoa, G. B.; Pedroso, E.; Moreno, V.; Grandas, A. *J. Biol. Inorg. Chem.* **1999**, *4*, 701.
(18) Hahn, M.; Kleine, M.; Sheldrick, W. S. *J. Biol. Inorg. Chem.* **2001**, *6*, 556.
(19) Saudek, V.; Pivcová, H.; Nosková, D.; Drobník, J. *J. Inorg. Biochem.* **1985**, *23*, 55.
(20) Appleton, T. G.; Pescb, F. J.; Wienken, M.; Menzer, S.; Lippert, B. *Inorg. Chem.* **1992**, *31*, 4410.
(21) Talebian, A. H.; Bensely, D.; Ghiorghis, A.; Hammer, C. F.; Schein, P. S.; Green, D. *Inorg. Chim. Acta* **1991**, *179*, 281.
(22) Appleton, T. G.; Hall, J. R.; Neale, D. W.; Thompson, C. S. M. *Inorg. Chem.* **1990**, *29*, 3985.
(23) Miller, S. E.; House, D. A. *Inorg. Chim. Acta* **1991**, *187*, 125.
(24) Kushev, D.; Gorneva, G.; Enchev, V.; Naydenova, E.; Popova, J.; Taxirov, S.; Maneva, L.; Grancharov, K.; Spassovska, N. *J. Inorg. Biochem.* **2002**, *89*, 203.
(25) Hindmarsh, K.; House, D. A.; Turnbull, M. M. *Inorg. Chim. Acta* **1997**, *257*, 11.
(26) Arpalahti, J.; Mikola, M.; Mauristo, S. *Inorg. Chem.* **1993**, *32*, 3327.
(27) Mikola, M.; Arpalahti, J. *Inorg. Chem.* **1994**, *33*, 4439.
(28) Martin, R. B. "Platinum Complexes and Binding to N(7) and N(1) of Purines." In *Cisplatin*; Lippert, B., (ed.); Wiley-VCH: Weinheim, 1999; pp 183.
(29) Berners-Price, S. J.; Frenkiel, T. A.; Frey, U.; Randolf, J. D.; Sadler, P. J. *J. Chem. Soc., Chem. Commun.* **1992**, 789.
(30) Orton, D. M.; Gretton, V. A.; Green, M. *Inorg. Chim. Acta* **1993**, *204*, 265.
(31) Appleton, T. G.; Bailey, A. J.; Barnham, K. J.; Hall, J. R. *Inorg. Chem.* **1992**, *31*, 3077.
(32) Mikola, M.; Arpalahti, J. *Inorg. Chem.* **1996**, *35*, 7556.
(33) Wilkins, R. G. *Kinetics and Mechanism of Reactions of Transition Metal Complexes*; VCH: Weinheim, 1991; Vol. Chapter 4.
(34) Schmuelling, M.; Lippert, B.; van Eldik, R. *Inorg. Chem.* **1994**, *33*, 3276.

(35) Bancroft, D. P.; Lepre, C. A.; Lippard, S. J. *J. Am. Chem. Soc.* **1990**, *112*, 6860.
(36) Bernges, F.; Doerner, G.; Holler, E. *Eur. J. Biochem.* **1990**, *191*, 743.
(37) Bernges, F.; Holler, E. *Nucleic Acids Res.* **1991**, *19*, 1483.
(38) Arpalahti, J. "Platinum(II)-Nucleobase Interactions. A Kinetic Approach." In *Metal Ions in Biological Systems*; Sigel A., Sigel H., (eds.); Marcel Dekker, Inc.: New York, Basel, Hong Kong, 1996; Vol. 32; pp 380.
(39) Jestin, J.-L.; Lambert, B.; Chottard, J.-C. *J. Biol. Inorg. Chem.* **1998**, *3*, 515.
(40) Mudroch, P. d. S.; Guo, Z.; Parkinson, J. A.; Sadler, P. J. *J. Biol. Inorg. Chem.* **1999**, *4*, 32.
(41) Lemma, K.; Berglund, J.; Farell, N.; Elding, L. I. *J. Biol. Inorg. Chem.* **2000**, *5*, 300.
(42) Lipinski, J. *Journal of Mol. Struct. (Theochem)* **1989**, *201*, 295.
(43) Basch, H.; Krauss, M.; Stevens, W. J.; Cohen, D. *Inorg. Chem.* **1986**, *25*, 684.
(44) Kozelka, J.; Chottard, J.-C. *Biophys. Chemistry* **1990**, *35*, 165.
(45) Kozelka, J.; Savinelli, R.; Berthier, G.; Flament, J.-P.; Lavery, R. *J. Comput. Chem.* **1993**, *14*, 45.
(46) Kozelka, J. "Molecular Modeling of Transition Metal Complexes with Nucleic Acids and Their Constituents." In *Metal Ions in Biological Systems*; Sigel A., Sigel. H., (eds.); Marcel Dekker, Inc.: New York, Basel, Hong Kong, 1996; Vol. 33; pp 2.
(47) Elizondo-Riojas, M. A.; Kozelka, J. *J. Mol. Biol.* **2001**, *314*, 1227.
(48) Pavankumar, P. N.; Seetharamulu, P.; Yao, S.; Saxe, J. D.; Reddy, D. G.; Hausheer, F. H. *J. Comput. Chem.* **1999**, *20*, 365.
(49) Carloni, P.; Andreoni, W.; Hutter, J.; Curioni, A.; Giannozzi, P.; Parrinello, M. *Chem. Phys. Letters* **1995**, *234*, 50.
(50) Carloni, P.; Andreoni, W. *J. Phys. Chem.* **1996**, *100*, 17797.
(51) Tornaghi, E.; Andreoni, W.; Carloni, P.; Hutter, J.; Parrinello, M. *Chemical Physics Letters* **1995**, *246*, 469.
(52) Wysokinski, R.; Michalska, D. *J. Comp. Chem.* **2001**, *22*, 901.
(53) Chval, Z.; Šíp, M. *J. Mol. Struct. (THEOCHEM)* **2000**, *532*, 59.
(54) Carloni, P.; Sprik, M.; Andreoni, W. *J. Phys. Chem. B* **2000**, *104*, 823.
(55) Deubel, D. V. *J. Am.Chem. Soc.* **2004**, *126*, 5999.
(56) Deubel, D. V. *J. Am. Chem. Soc.* **2002**, *124*, 5834.
(57) Chval, Z.; Šíp, M. *Collection of Czechoslovak Chemical Communications* **2003**, *68*, 1105.
(58) Eriksson, L. A.; Raber, J.; Zhu, C. *J. Phys. Chem.* **2005**, 000.
(59) Hill, G. A.; Gorb, L.; Leszczynski, J. *Int. J. Quantum Chem.* **2002**, *90*, 1121.
(60) Spiegel, K.; Rothlisberger, U.; Carloni, P. *J. Phys. Chem. B* **2004**, *108*, 2699.
(61) Baik, M.-H.; Friesner, R. A.; Lippard, S. J. *J. Am. Chem. Soc.* **2002**, *124*, 4495.

(62) Baik, M. H.; Friesner, R. A.; Lippard, S. J. *Inorganic Chemistry* **2003**, *42*, 8615.
(63) Burda, J. V.; Leszczynski, J. *Inorg. Chem.* **2003**, *42*., 7162.
(64) Zeizinger, M.; Burda, J. V.; Leszczynski, J. *PCCP* **2004**, *6*, 3585.
(65) Šponer, J.; Šponer, J. E.; Gorb, L.; Leszczynski, J.; Lippert, B. *J. Phys. Chem. A* **1999**, *103*, 11406.
(66) Burda, J. V.; Šponer, J.; Leszczynski, J. *J. Biol. Inorg. Chem.* **2000**, *5*, 178.
(67) Burda, J. V.; Šponer, J.; Leszczynski, J. *Phys. Chem. Chem. Phys.* **2001**, *3*, 4404.
(68) Šponer, J. E.; Leszczynski, J.; Glahe, F.; Lippert, B.; Šponer, J. *Inorg. Chem.* **2001**, *40*, 3269.
(69) Šponer, J. E.; Sanz Miguel, J.; Rodriguez-Santiago, L.; Erxleben, A.; Krumm, M.; Sodupe, M.; Šponer, J.; Lippert, B. *Angew. Chem. Int. Ed. Engl.* **2004**, *43*, 5396.
(70) Curtiss, L. A.; Raghavachari, K.; Redfern, P. C.; Rassolov, V.; Pople, J. A. *J. Chem. Phys.* **1998**, *109*, 7764.
(71) Andrae, D.; Haussermann, U.; Dolg, M.; Stoll, H.; Preuss, H. *Theor. Chim. Acta* **1990**, *77*, 123.
(72) Kuechle, W.; Dolg, M.; Stoll, H.; Preuss, H. *J. Chem. Phys.* **1994**, *100*, 7535.
(73) Nicklass, A.; Dolg, M.; Stoll, H.; Preuss, H. *J. Chem. Phys.* **1995**, *102*, 8942.
(74) LaJohn, L. A.; Christiansen, P. A.; Ross, R. B.; Atashroo, T.; Ermler, W. C. *J. Chem. Phys.* **1987**, *87*, 2812.
(75) Ross, R. B.; Powers, J. M.; Atashroo, T.; Ermler, W. C.; LaJohn, L. A.; Christiansen, P. A. *J. Chem. Phys.* **1990**, *93*, 6654.
(76) Burda, J. V.; Runenberg, N.; Pyykko, P. *Chem. Phys. Letters* **1998**, *288*, 635.
(77) Pitzer, R. M.; Winter, N. W. *J. Phys. Chem.* **1988**, *92*, 3061.
(78) Pitzer, R. M.; Winter, N. W. *Int. J. Quantum Chem.* **1991**, *40*, 773.
(79) Pitzer, R. M. "OSU-TCG Report," OSU-TCG Report, 1991.
(80) Pitzer, R. M. S-O version of program COLUMBUS: Ohio state University, 1990.
(81) Werner, H. J.; Knowles, P. J. MOLPRO 98 University of Sussex, UK, 1998.
(82) Blaise, J.; Verges, J.; Wyart, J.-F.; Engleman, Jr., R. *J. Res. Natl. Inst. Stand. Technol.* **1992**, *97*, 213.
(83) Böhme, M.; Frenklin, G. *Chem. Phys. Letters* **1994**, *224*, 195.
(84) Hrušák, J.; Ten-no, S.; Iwata, S. *J. Chem. Phys.* **1997**, *106*, 7185.
(85) Fuentealba, P.; Preuss, H.; Hermann, S.; Von Szentpaly, L. *Chem. Phys. Letters* **1982**, *89*, 418.
(86) Müller, W.; Fleisch, J.; Meyer, W. *J. Chem. Phys.* **1984**, *80*, 3297.
(87) Huzinaga, S.; Miguel, B. *Chem. Phys. Letters* **1990**, *175*, 289.
(88) Huzinaga, S.; Klobukowski, M. *Chem. Phys. Letters* **1993**, *212*, 260.
(89) Desclaux, J. P. *Data and Nuclear Data ables* **1973**, *12*, 311.
(90) Parr, R. G.; Pearson, R. G. *J. Am. Chem. Soc.* **1983**, *105*, 7512.

(91) Colacio, E.; Cuesta, R.; Ghazi, M.; Huertas, M. A.; Moreno, J. M.; Navarrete, A. *Inorg. Chem.* **1997**, *36*, 1652.
(92) Efimenko, I. A.; Kurbakova, A. P.; Mativic, Z. D.; Ponticelli, G. *Transition Metal Chem.* **1994**, *19*, 539.
(93) Efimenko, I. A.; Kurbakova, A. P.; Mativic, Z. D.; Ponticelli, G. *Transition Metal Chem.* **1994**, *19*, 640.
(94) Bray, M. R.; Deeth, R. J.; Paget, V. J.; Sheen, P. D. *Int. J. Quantum Chem.* **1996**, *61*, 85.
(95) Deeth, R. J. *Chem. Phys. Lett.* **1996**, *261*, 45.
(96) Deeth, R. J.; Jenkins, H. D. B. *J. Phys. Chem. A* **1997**, *101*, 4793.
(97) Swang, O.; Blom, R.; Ryan, O. B.; Faegri, Jr., K. *J. Phys. Chem.* **1996**, *100*, 17334.
(98) *Comprehensive Organometallic Chemistry II*; Pergamon: Oxford, 1995; Vol. 9.
(99) Garmer, D. R.; Gresh, N. *J. Am. Chem. Soc.* **1994**, *116*, 3556.
(100) Gresh, N.; Garmer, D. R. *J. Comput. Chem.* **1996**, *17*, 1481.
(101) Šponer, J.; Burda, J. V.; Sabat, M.; Leszczynski, J.; Hobza, P. *J. Phys. Chem. A* **1998**, *102*, 5951.
(102) Hill, G.; Gora, R. W.; Roszak, S.; Leszczynki, J. *Int. J. Quantum Chem.* **2001**, *83*, 213.
(103) Hay, P. J.; Wadt, W. R. *J. Chem. Phys.* **1985**, *82*, 270.
(104) Kirik, S. D.; Solovyov, L. A.; Bokhin, A. I.; Yakimov, I. S.; Blokhina, M. L. *Acta Cryst. B.* **1996**, *52*, 909.
(105) Ma, Y. G.; Politzer, P. *Journal of Chemical Physics* **2004**, *120*, 3152.
(106) Politzer, P.; Murray, J. S.; Lane, P. *Journal of Computational Chemistry* **2003**, *24*, 505.
(107) Politzer, P.; Murray, J. S. *Theoretical Chemistry Accounts* **2002**, *108*, 134.
(108) Politzer, P.; Grice, M. E.; Murray, J. S. *Journal of Molecular Structure-Theochem* **2001**, *549*, 69.
(109) Gresh, N. *J. Comput. Chem.* **1995**, *16*, 856.
(110) Zhang, Y.; Guo, Z.; You, X.-Z. *J. Am. Chem. Soc.* **2001**, *123*, 9378.
(111) Costa, L. A. S.; Rocha, W. R.; De Almeida, W. B.; Dos Santos, H. F. *J. Chem. Phys.* **2003**, *118*, 10584.
(112) Costa, L. A. S.; Rocha, W. R.; De Almeida, W. B.; Dos Santos, H. F. *Chem. Phys. Letters* **2004**, *387*, 182.
(113) Robertazzi, A.; Platts, J. A. *Journal of Computational Chemistry* **2004**, *25*, 1060.
(114) Peng, C.; Ayala, P. Y.; Schlegel, H. B.; Frisch, M. J. *J. Comput. Chem.* **1996**, *17*, 49.
(115) Bergner, A.; Dolg, M.; Kuechle, W.; Stoll, H.; Preuss, H. *Mol. Phys.* **1993**, *80*, 1431.
(116) Dolg, M.; Stoll, H.; Preuss, H.; Pitzer, R. M. *J. Phys. Chem.* **1993**, *97*, 5852.

(117) Urban, M.; Hobza, P. *Theor. Chim. Acta* **1975**, *36*, 215.
(118) Boys, S. F.; Bernardi, F. *Mol. Phys.* **1970**, *19*, 553.
(119) Smedarchina, Z.; Fernández-Ramos, A.; Siebrand, W. *J. Comput. Chem.* **2001**, *22*, 787.
(120) Schnebeck, R.-D.; Freisinger, E.; Glahe, F.; Lippert, B. *J. Am. Chem. Soc.* **2000**, *122*, 1381.
(121) Pierloot, K.; Ceulemans, A.; Merchan, M.; Serrano-Andres, L. *J. Phys. Chem. A* **2000**, *104*, 4374.
(122) Hartley, F. R. *The Chemistry of Platinum and Palladium*; Applied Science Publishers Ltd.: London, 1973.
(123) Aragoni, M. C.; Arca, M.; Demartin, F.; Devillanova, F. A.; Garau, A.; Isaia, F.; Lelj, F.; Lippolis, V.; Verani, G. *J. Am. Chem. Soc.* **1999**, *121*, 7098.
(124) Legendre, F.; Chottard, J.-C. "Kinetics and Selectivity of DNA-Platination." In *Cisplatin*; Lippert, B., (ed.); Wiley-VCH: Weinheim, 1999.
(125) Kuo, L. Y.; Liu, A. H.; Marks, T. J. "Metallocene Interactions with DNA and DNA-Processing Enzymes." In *Metal Ions in Biological Systems*; Sigel, A. Sigel H.., (eds.); Marcel Dekker, Inc.: New York, Basel, Hong Kong, 1995; Vol. 33; pp 53.
(126) Burda, J. V.; Šponer, J.; Hrabáková, J.; Zeizinger, M.; Leszczynski, J. *J. Phys. Chem. B* **2003**, *107*, 5349.
(127) Tomasi, J.; Cammi, R.; Mennucci, B.; Cappelli, C.; Corni, S. *PCCP* **2002**, *4*, 5697.
(128) Klamt, A.; Eckert, F.; Hornig, M.; Beck, M. E.; Burger, T. *J. Comp. Chem.* **2002**, *23*, 275.
(129) Tomasi, J.; Cammi, R.; Mennucci, B. *Int. J. Quantum Chem.* **1999**, *775*, 7783.
(130) Amovilli, C.; Barone, V.; Cammi, R.; Cancès, E.; Cossi, M.; Mennucci, B.; Pomelli, C. S.; Tomasi, J. *Advances in Quantum Chemistry* **1998**, *32*, 227.
(131) Bonaccorsi, R.; Palla, P.; Tomasi, J. *J. Am. Chem. Soc.* **1984**, *106*, 1945.
(132) Barone, V.; Adamo, C.; Grand, A.; Subra, R. *Chem. Phys. Letters* **1995**, *242*, 351.
(133) Nielsen, P. A.; Norrby, P. O.; Liljefors, T.; Rega, N.; Barone, V. *J. Am. Chem. Soc.* **2000**, *122*, 3151.
(134) Segal-Bendirdjian, E.; Brehin, P.; Lambert, B.; Laousi, A.; Kozelka, J.; Barreau, M.; Lavalle, F.; LePecq, J. B.; Chottard, J.-C. *Platinum and other metal coordination compounds in cancer chemotherapy*; Plenum Press: New York, 1991.
(135) Johnson, N. P.; Hoeschele, J. D.; Rahn, R. O. *Chemico-Biological Interactions* **1980**, *30*, 151.
(136) Gelasco, A.; Lippard, S. J. *Biochemistry* **1998**, *37*, 9230.